

Bringing Light Into the Dark: A Large-scale Evaluation of Knowledge Graph Embedding Models under a Unified Framework

Mehdi Ali, Max Berrendorf[†], Charles Tapley Hoyt[†], Laurent Vermue[†], Mikhail Galkin,
Sahand Sharifzadeh, Asja Fischer, Volker Tresp, and Jens Lehmann

Abstract—The heterogeneity in recently published knowledge graph embedding models’ implementations, training, and evaluation has made fair and thorough comparisons difficult. To assess the reproducibility of previously published results, we re-implemented and evaluated 19 models in the PyKEEN software package. In this paper, we outline which results could be reproduced with their reported hyper-parameters, which could only be reproduced with alternate hyper-parameters, and which could not be reproduced at all, as well as provide insight as to why this might be the case.

We then performed a large-scale benchmarking on four datasets with several thousands of experiments and 21,246 GPU hours of computation time. We present insights gained as to best practices, best configurations for each model, and where improvements could be made over previously published best configurations. Our results highlight that the combination of model architecture, training approach, loss function, and the explicit modeling of inverse relations is crucial for a model’s performance and is not only determined by its architecture. We provide evidence that several architectures can obtain results competitive to the state of the art when configured carefully. We have made all code, experimental configurations, results, and analyses available at <https://github.com/pykeen/pykeen> and <https://github.com/pykeen/benchmarking>.

Index Terms—Knowledge Graph Embeddings, Link Prediction, Reproducibility, Benchmarking

I. INTRODUCTION

AS the usage of knowledge graphs (KGs) becomes more widespread, their inherent incompleteness can pose a liability for typical downstream tasks that they support, e.g., question answering, dialogue systems, and recommendation systems [1]. Knowledge graph embedding models (KGEMs) present an avenue for predicting missing links. However, the following two major challenges remain in their application.

[†]Equal contribution.

Mehdi Ali is affiliated with Smart Data Analytics (University of Bonn), Germany, & Fraunhofer IAIS, Sankt Augustin and Dresden, Germany.

Max Berrendorf is affiliated with Ludwig-Maximilians-Universität München, Munich, Germany.

Charles Tapley Hoyt is affiliated with Enveda Therapeutics, Bonn, Germany.

Laurent Vermue is affiliated with the Technical University of Denmark, Kongens Lyngby, Denmark.

Mikhail Galkin is affiliated with the Technical University of Dresden, Germany, & Fraunhofer IAIS, Sankt Augustin and Dresden, Germany.

Sahand Sharifzadeh is affiliated with Ludwig-Maximilians-Universität München, Munich, Germany.

Asja Fischer is affiliated with the Ruhr University Bochum, Germany.

Volker Tresp is affiliated with Ludwig-Maximilians-Universität München & Siemens AG, Munich, Germany.

Jens Lehmann is affiliated with Smart Data Analytics (University of Bonn), Bonn, Germany, & Fraunhofer IAIS, Sankt Augustin and Dresden Germany.

First, the reproduction of previously reported results turned out to be a major challenge — there are even examples of different results reported for the same combinations of KGEMs and datasets [2]. In some cases, the lack of availability of source code for KGEMs or the usage of different frameworks and programming languages inevitably introduces variability. In other cases, the lack of a precise specification of hyper-parameters introduces variability.

Second, the verification of the novelty of previously reported results remains difficult. It is often difficult to attribute the incremental improvements in performance reported with each new state of the art model to the model’s architecture itself or instead to the training approach, hyper-parameter values, or specific preprocessing steps, e.g., the explicit modeling of inverse relations. It has been shown that baseline models can achieve competitive performance to more sophisticated ones when optimized appropriately [3], [2]. Additionally, the variety of implementations and interpretations of common evaluation metrics for link prediction makes a fair comparison to previous results difficult [4].

This paper makes two major contributions towards addressing these challenges:

- 1) We performed a reproducibility study in which we tried to replicate reported experimental results in the original papers (when sufficient information was provided).
- 2) We performed an extensive benchmark study on 19 KGEMs over four benchmark datasets in which we evaluated the models based on different hyper-parameter values, training approaches (i.e. training under the *local closed world assumption* and *stochastic local closed world assumption*), loss functions, optimizers, and the explicit modeling of inverse relations.

Previous studies have already investigated important aspects for a subset of models: Kadlec *et al.* [3] showed that a fine-tuned baseline (DistMult [5]) can outperform more sophisticated models on FB15K. Akrami *et al.* [2], [6] examined the effect of removing faulty triples from KGs on the model’s performance. Mohamed *et al.* [7] studied the influence of loss functions on the models’ performances for a set of KGEMs. Concurrent to the work on this paper, Rufinelli *et al.* [8] performed a benchmarking study in which they investigated ve knowledge graph embedding models. After describing their benchmarking [8], they called for a larger study that extends the search space and incorporates more sophisticated models.

Our study answers this call and realizes a fair benchmarking by completely re-implementing KGEMs, training pipelines, loss functions, regularizations, and evaluation metrics in a unified, open-source framework. Inspired by their findings, we have also included the cross entropy loss (CEL) function, which has been previously used by Kadlec *et al.* [3]. Our benchmarking can be considered as a superset of many previous benchmarkings — to the best of our knowledge, there exists no study of comparable breadth or depth. A further interesting study with a different focus is the work of Rossi *et al.* [9] in which they investigated the effect of the structural properties of KGs on models’ performances, instead of focusing on the combinations of different model architectures, training approaches, and loss functions.

This article is structured as follows: in Section II, we introduce our notation of KG and the link prediction task and introduce an exemplary KG to which we refer in examples throughout this paper. In Section III, we present our definition of a KGEM and review the KGEMs that we investigated in our studies. In Section IV, we describe and discuss established evaluation metrics as well as a recently proposed one [10]. In Section V, we introduce the benchmark datasets on which we conducted our experiments. In Section VI and Section VII, we present our respective reproducibility and benchmarking studies. Finally, we provide a discussion and an outlook for our future work in Section VIII.

II. KNOWLEDGE GRAPHS

For a given set of entities \mathcal{E} and set of relations \mathcal{R} , we consider a knowledge graph $\mathcal{K} \subseteq \mathbb{K} = \mathcal{E} \times \mathcal{R} \times \mathcal{E}$ as a directed, multi-relational graph that comprises triples $(h, r, t) \in \mathcal{K}$ in which $h, t \in \mathcal{E}$ represent a triples’ respective head and tail entities and $r \in \mathcal{R}$ represents its relationship. Figure 1 depicts an exemplary KG and Table I a subset of its triples. The direction of a relationship indicates the roles of the entities, i.e., head or tail entity. For instance, in the triple $(\text{Sarah}, \text{CEO_Of}, \text{Deutsche_Bank})$, *Sarah* is the head and *Deutsche_Bank* is the tail entity. KGs usually contain only true triples corresponding to available knowledge.

In contrast to triples in a KG, there are different philosophies, or *assumptions*, for the consideration of triples *not* contained in a KG [11], [12]. Under the closed world assumption (CWA), all triples that are not part of a KG are considered as false. Based on the example in Figure 1, the triple $(\text{Sarah}, \text{lives_in}, \text{Germany})$ is a false fact under the CWA since it is not part of the KG. Under the open world assumption (OWA), it is considered unknown as to whether triples that are not part of the KG are true or false. The construction of KGs under the principles of the semantic web (and RDF) rely on the OWA as well as most of the relevant works to this paper [13], [11].

Because KGs are usually incomplete and noisy, several approaches have been developed to predict new links. In particular, the task of link prediction is defined as predicting the tail/head entities for $(h, r)/(r, t)$ pairs. For instance, given queries of the form $(\text{Sarah}, \text{studied_at}, ?)$ or $(?, \text{CEO_of}, \text{Deutsche_Bank})$, the task is the correctly detect the entities that answer the query, i.e. $(\text{Sarah}, \text{studied_at}, \text{University})$

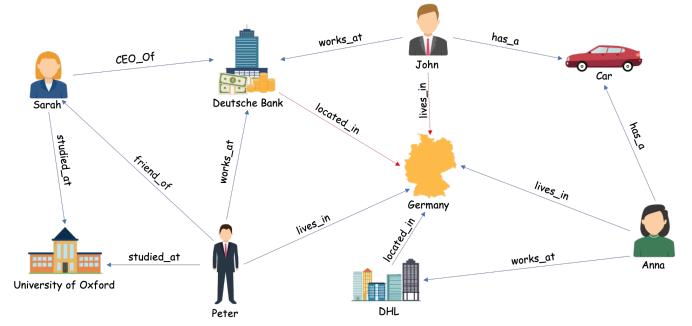


Fig. 1. Exemplary KG: nodes represent entities and edges their respective relations.

TABLE I
SUBSET OF TRIPLES OF THE EXEMPLARY KG.

Head	Relation	Tail
Sarah	CEO_Of	Deutsche Bank
Sarah	studied_at	University of Oxford
Peter	friend_of	Sarah
Peter	works_at	Deutsche Bank
Peter	studied_at	University of Oxford
Peter	lives_in	Germany

of Oxford) and $(\text{Sarah}, \text{CEO_of}, \text{Deutsche_Bank})$. While classical approaches have relied on domain-specific rules to derive missing links, they usually require a large number of user-defined rules in order to generalize [11]. Alternatively, machine learning approaches learn to predict new links based on the set of existing ones. It has been shown that especially relational-machine learning methods are successful in predicting missing links and identifying incorrect ones, and recently knowledge graph embedding models have gained significant attention [11].

III. KNOWLEDGE GRAPH EMBEDDING MODELS

Knowledge graph embedding models (KGEMs) learn latent vector representations of the entities $e \in \mathcal{E}$ and relations $r \in \mathcal{R}$ in a KG that best preserve its structural properties [1], [11]. Besides for link prediction, they have been used for tasks such as entity disambiguation, and clustering as well as for downstream tasks such as question answering, recommendation systems, and relation extraction [1]. Figure 2 shows an embedding of the entities and relations in \mathbb{R}^2 from the KG from Figure 1.

Here, we define a KGEM as four components: an *interaction model*, a *training approach*, a *loss function*, and its usage of *explicit inverse relations*. This abstraction enables investigation of the effect of each component individually and in combination on each KGEMs’ performance. Each are described in detail in their following respective subsections III-A, III-B, III-C, and III-D.

In this paper, we use a boldface lower-case letter \mathbf{x} to denote a vector, $\|\mathbf{x}\|_p$ to represent its l_p norm, a boldface upper-case letter \mathbf{X} to denote a matrix, and a fraktur-font upper-case letter \mathfrak{X} to represent a three-mode tensor. Furthermore, we use \odot to denote the Hadamard product $\odot : \mathbb{R}^d \times \mathbb{R}^d \rightarrow \mathbb{R}^d$:

$$\mathbf{t}_r = \mathbf{M}_{r,t} \mathbf{t} . \quad (14)$$

Finally, the plausibility score for $(h, r, t) \in \mathbb{K}$ is given by:

$$f(h, r, t) = -\|\mathbf{h}_r + \mathbf{r} - \mathbf{t}_r\|_2^2 . \quad (15)$$

g) **RESCAL**: RESCAL [20] is a bilinear model that models entities as vectors and relations as matrices. The relation matrices $\mathbf{W}_r \in \mathbb{R}^{d \times d}$ contain weights $w_{i,j}$ that capture the amount of interaction between the i -th latent factor of $\mathbf{h} \in \mathbb{R}^d$ and the j -th latent factor of $\mathbf{t} \in \mathbb{R}^d$ [11], [20]. Thus, the plausibility score of $(h, r, t) \in \mathbb{K}$ is given by:

$$f(h, r, t) = \mathbf{h}^T \mathbf{W}_r \mathbf{t} = \sum_{i=1}^d \sum_{j=1}^d w_{ij}^{(r)} h_i t_j \quad (16)$$

h) **DistMult**: DistMult [5] is a simplification of RESCAL where the relation matrices $\mathbf{W}_r \in \mathbb{R}^{d \times d}$ are restricted to diagonal matrices:

$$f(h, r, t) = \mathbf{h}^T \mathbf{W}_r \mathbf{t} = \sum_{i=1}^d \mathbf{h}_i \cdot \text{diag}(\mathbf{W}_r)_i \cdot \mathbf{t}_i . \quad (17)$$

Because of its restriction to diagonal matrices DistMult is computational more efficient than RESCAL, but at the same time less expressive. For instance, it is not able to model anti-symmetric relations, since $f(h, r, t) = f(t, r, h)$.

i) **Complex**: ComplEx [21] is an extension of DistMult that uses complex valued representations for the entities and relations. Entities and relations are represented as vectors $\mathbf{h}, \mathbf{r}, \mathbf{t} \in \mathbb{C}^d$, and the plausibility score is computed using the Hadamard product:

$$\begin{aligned} f(h, r, t) &= \text{Re}(\mathbf{h} \odot \mathbf{r} \odot \mathbf{t}) \\ &= \langle \text{Re}(\mathbf{h}), \text{Re}(\mathbf{r}), \text{Re}(\mathbf{t}) \rangle \\ &\quad + \langle \text{Im}(\mathbf{h}), \text{Re}(\mathbf{r}), \text{Im}(\mathbf{t}) \rangle \\ &\quad + \langle \text{Re}(\mathbf{h}), \text{Re}(\mathbf{r}), \text{Im}(\mathbf{t}) \rangle \\ &\quad - \langle \text{Im}(\mathbf{h}), \text{Im}(\mathbf{r}), \text{Im}(\mathbf{t}) \rangle , \end{aligned} \quad (18)$$

where $\text{Re}(\mathbf{x})$ and $\text{Im}(\mathbf{x})$ denote the real and imaginary parts of the complex valued vector \mathbf{x} . Because the Hadamard product is not commutative in the complex space, ComplEx can model anti-symmetric relations in contrast to DistMult.

j) **RotatE**: RotatE [22] models relations as rotations from head to tail entities in the complex space:

$$\mathbf{t} = \mathbf{h} \odot \mathbf{r} , \quad (19)$$

where $\mathbf{h}, \mathbf{r}, \mathbf{t} \in \mathbb{C}^d$ and $|r_i| = 1$, that is the complex elements of \mathbf{r} are restricted to have a modulus of one. Because of the latter, r_i can be represented as $e^{i\theta_{r,i}}$, which corresponds to a counterclockwise rotation by $\theta_{r,i}$ radians. The interaction model is then defined as:

$$f(h, r, t) = -\|\mathbf{h} \odot \mathbf{r} - \mathbf{t}\| , \quad (20)$$

which allows to model *symmetry*, *antisymmetry*, *inversion*, and *composition* [22].

k) **Simple**: Simple [23] is an extension of **canonical polyadic (CP)** [23], one of the early tensor factorization approaches. In CP, each entity $e \in \mathcal{E}$ is represented by two vectors $\mathbf{h}_e, \mathbf{t}_e \in \mathbb{R}^d$ and each relation by a single vector $\mathbf{r} \in \mathbb{R}^d$. Depending whether an entity participates in a triple as the head or tail entity, either \mathbf{h}_e or \mathbf{t}_e is used. Both entity representations are learned independently, i.e. observing a triple (e_1, r, e_2) , the method only updates \mathbf{h}_{e_1} and \mathbf{t}_{e_2} . In contrast to CP, Simple introduces for each relation r the inverse relation r' , and formulates the interaction model based on both:

$$f(h, r, t) = \frac{1}{2} (\langle \mathbf{h}_{e_1}, \mathbf{r}, \mathbf{t}_{e_2} \rangle + \langle \mathbf{h}_{e_2}, \mathbf{r}', \mathbf{t}_{e_1} \rangle) . \quad (21)$$

Therefore, for each triple $(e_1, r, e_2) \in \mathbb{K}$, both \mathbf{h}_{e_1} and \mathbf{t}_{e_2} as well as \mathbf{h}_{e_2} and \mathbf{t}_{e_1} are updated [23].

l) **Tucker**: Tucker [24] is a linear model that is based on the tensor factorization method Tucker [25] in which a three-mode tensor $\mathfrak{X} \in \mathbb{R}^{I \times J \times K}$ is decomposed into a set of factor matrices $\mathbf{A} \in \mathbb{R}^{I \times P}$, $\mathbf{B} \in \mathbb{R}^{J \times Q}$, and $\mathbf{C} \in \mathbb{R}^{K \times R}$ and a core tensor $\mathfrak{Z} \in \mathbb{R}^{P \times Q \times R}$ (of lower rank):

$$\mathfrak{X} \approx \mathfrak{Z} \times_1 \mathbf{A} \times_2 \mathbf{B} \times_3 \mathbf{C} , \quad (22)$$

where \times_n is the tensor product, with n denoting along which mode the tensor product is computed. In Tucker, a KG is considered as a binary tensor which is factorized using the Tucker factorization where $\mathbf{E} = \mathbf{A} = \mathbf{C} \in \mathbb{R}^{n_e \times d_e}$ denotes the entity embedding matrix, $\mathbf{R} = \mathbf{B} \in \mathbb{R}^{n_r \times d_r}$ represents the relation embedding matrix, and $\mathfrak{W} = \mathfrak{Z} \in \mathbb{R}^{d_e \times d_r \times d_e}$ is the *core tensor* that indicates the extent of interaction between the different factors. The interaction model is defined as:

$$f(h, r, t) = \mathfrak{W} \times_1 \mathbf{h} \times_2 \mathbf{r} \times_3 \mathbf{t} , \quad (23)$$

where \mathbf{h}, \mathbf{t} correspond to rows of \mathbf{E} and \mathbf{r} to a row of \mathbf{R} .

m) **ProjE**: ProjE [26] is a neural network-based approach with a *combination* and a *projection* layer. The interaction model first combines h and r by following combination operator [26]:

$$\mathbf{h} \otimes \mathbf{r} = \mathbf{D}_e \mathbf{h} + \mathbf{D}_r \mathbf{r} + \mathbf{b}_c , \quad (24)$$

where $\mathbf{D}_e, \mathbf{D}_r \in \mathbb{R}^{k \times k}$ are diagonal matrices which are used as shared parameters among all entities and relations, and $\mathbf{b}_c \in \mathbb{R}^k$ represents the candidate bias vector shared across all entities. Next, the score for the triple $(h, r, t) \in \mathbb{K}$ is computed:

$$f(h, r, t) = g(\mathbf{t} z(\mathbf{h} \otimes \mathbf{r}) + \mathbf{b}_p) , \quad (25)$$

where g and z are activation functions, and \mathbf{b}_p represents the shared projection bias vector.

n) **HolE**: Holographic embeddings (HolE) [27] make use of the circular correlation operator to compute interactions between latent features of entities and relations:

$$f(h, r, t) = \sigma(\mathbf{r}^T (\mathbf{h} \star \mathbf{t})) . \quad (26)$$

where the circular correlation $\star : \mathbb{R}^d \times \mathbb{R}^d \rightarrow \mathbb{R}^d$ is defined as:

$$[\mathbf{a} \star \mathbf{b}]_i = \sum_{k=0}^{d-1} \mathbf{a}_k \star \mathbf{b}_{(i+k) \bmod d} \quad (27)$$

By using the correlation operator each component $[\mathbf{h} \star \mathbf{t}]_i$ represents a sum over a fixed partition over pairwise interactions. This enables the model to put semantic similar interactions into the same partition and share weights through \mathbf{r} . Similarly irrelevant interactions of features could also be placed into the same partition which could be assigned a small weight in \mathbf{r} .

o) KG2E: KG2E [28] aims to explicitly model (un)certainties in entities and relations (e.g. influenced by the number of triples observed for these entities and relations). Therefore, entities and relations are represented by probability distributions, in particular by multi-variate Gaussian distributions $\mathcal{N}_i(\boldsymbol{\mu}_i, \boldsymbol{\Sigma}_i)$ where the mean $\boldsymbol{\mu}_i \in \mathbb{R}^d$ denotes the position in the vector space and the diagonal variance $\boldsymbol{\Sigma}_i \in \mathbb{R}^{d \times d}$ models the uncertainty. Inspired by the TransE model, relations are modeled as transformations from head to tail entities: $\mathcal{H} - \mathcal{T} \approx \mathcal{R}$ where $\mathcal{H} \sim \mathcal{N}_h(\boldsymbol{\mu}_h, \boldsymbol{\Sigma}_h)$, $\mathcal{H} \sim \mathcal{N}_t(\boldsymbol{\mu}_t, \boldsymbol{\Sigma}_t)$, $\mathcal{R} \sim \mathcal{P}_r = \mathcal{N}_r(\boldsymbol{\mu}_r, \boldsymbol{\Sigma}_r)$ and $\mathcal{H} - \mathcal{T} \sim \mathcal{P}_e = \mathcal{N}_{h-t}(\boldsymbol{\mu}_h - \boldsymbol{\mu}_t, \boldsymbol{\Sigma}_h + \boldsymbol{\Sigma}_t)$ (since head and tail entities are considered to be independent with regards to the relations). The interaction model measures the similarity between \mathcal{P}_e and \mathcal{P}_r by means of the Kullback-Leibler (KL) divergence:

$$\begin{aligned} f(h, r, t) &= \mathcal{D}_{\mathcal{KL}}(\mathcal{P}_e, \mathcal{P}_r) \\ &= \frac{1}{2} \left\{ \text{tr}(\boldsymbol{\Sigma}_r^{-1} \boldsymbol{\Sigma}_e) + (\boldsymbol{\mu}_r - \boldsymbol{\mu}_e)^T \boldsymbol{\Sigma}_r^{-1} (\boldsymbol{\mu}_r - \boldsymbol{\mu}_e) \right. \\ &\quad \left. - \log\left(\frac{\det(\boldsymbol{\Sigma}_e)}{\det(\boldsymbol{\Sigma}_r)}\right) - d \right\}. \end{aligned} \quad (28)$$

Besides the asymmetric KL divergence, the authors propose a symmetric variant which uses the expected likelihood:

$$\begin{aligned} f(h, r, t) &= \log \mathcal{D}_{\mathcal{EL}}(\mathcal{P}_e, \mathcal{P}_r) \\ &= \frac{1}{2} \left\{ (\boldsymbol{\mu}_e - \boldsymbol{\mu}_r)^T (\boldsymbol{\Sigma}_e + \boldsymbol{\Sigma}_r)^{-1} (\boldsymbol{\mu}_e - \boldsymbol{\mu}_r) \right. \\ &\quad \left. + \log \det(\boldsymbol{\Sigma}_e + \boldsymbol{\Sigma}_r) + k_e \log(2\pi) \right\}. \end{aligned} \quad (29)$$

p) ERMLP: ERMLP [29] is a multi-layer perceptron based approach that uses a single hidden layer and represents entities and relations as vectors. In the input-layer, for each triple the embeddings of head, relation, and tail are concatenated and passed to the hidden layer. The output-layer consists of a single neuron that computes the plausibility score of the triple:

$$f(h, r, t) = \mathbf{w}^T g(\mathbf{W}[\mathbf{h}; \mathbf{r}; \mathbf{t}]), \quad (30)$$

where $\mathbf{W} \in \mathbb{R}^{k \times 3d}$ represents the weight matrix of the hidden layer, $\mathbf{w} \in \mathbb{R}^k$, the weights of the output layer, and g denotes an activation function such as the hyperbolic tangent.

q) Neural Tensor Network: The Neural Tensor Network (NTN) [30] uses a bilinear tensor layer instead of a standard linear neural network layer:

$$f(h, r, t) = \mathbf{u}_r^T \cdot \tanh(\mathbf{h} \mathbb{W}_r \mathbf{t} + \mathbf{V}_r [\mathbf{h}; \mathbf{t}] + \mathbf{b}_r), \quad (31)$$

where $\mathbb{W}_r \in \mathbb{R}^{d \times d \times k}$ is the relation specific tensor, and the weight matrix $\mathbf{V}_r \in \mathbb{R}^{k \times 2d}$, the bias vector \mathbf{b}_r , and the weight vector $\mathbf{u}_r \in \mathbb{R}^k$ are the standard parameters of a neural network, which are also relation specific. The result of the tensor product $\mathbf{h} \mathbb{W}_r \mathbf{t}$ is a vector $\mathbf{x} \in \mathbb{R}^k$ where each entry x_i is computed based on the slice i of the tensor \mathbb{W}_r : $\mathbf{x}_i = \mathbf{h} \mathbb{W}_r^i \mathbf{t}$ [30]. As indicated by the interaction model,

NTN defines for each relation a separate neural network which makes the model very expressive, but at the same time computationally expensive.

r) ConvKB: ConvKB [31] uses a convolutional neural network (CNN) whose feature maps capture global interactions of the input. Each triple $(h, r, t) \in \mathbb{K}$ is represented as a input matrix $\mathbf{A} = [\mathbf{h}; \mathbf{r}; \mathbf{t}] \in \mathbb{R}^{d \times 3}$ in which the columns represent the embeddings for h, r and t . In the convolution layer, a set of convolutional filters $\boldsymbol{\omega}_i \in \mathbb{R}^{1 \times 3}$, $i = 1, \dots, \tau$, are applied on the input in order to compute for each dimension global interactions of the embedded triple. Each $\boldsymbol{\omega}_i$ is applied on every row of \mathbf{A} creating a feature map $\mathbf{v}_i = [v_{i,1}, \dots, v_{i,d}] \in \mathbb{R}^d$:

$$\mathbf{v}_i = g(\boldsymbol{\omega}_i \mathbf{A} + \mathbf{b}), \quad (32)$$

where $\mathbf{b} \in \mathbb{R}$ denotes a bias term and g an activation function which is employed element-wise. Based on the resulting feature maps $\mathbf{v}_1, \dots, \mathbf{v}_\tau$, the plausibility score of a triple is given by:

$$f(h, r, t) = [\mathbf{v}_1; \dots; \mathbf{v}_\tau] \cdot \mathbf{w}, \quad (33)$$

where $[\mathbf{v}_1; \dots; \mathbf{v}_\tau] \in \mathbb{R}^{\tau d \times 1}$ and $\mathbf{w} \in \mathbb{R}^{\tau d \times 1}$ is a shared weight vector. ConvKB may be seen as a restriction of ER-MLP with a certain weight sharing pattern in the first layer.

s) ConvE: ConvE [32] is a CNN-based approach. For each triple (h, r, t) , the input to ConvE is a matrix $\mathbf{A} \in \mathbb{R}^{2 \times d}$ where the first row of \mathbf{A} represents $\mathbf{h} \in \mathbb{R}^d$ and the second row represents $\mathbf{r} \in \mathbb{R}^d$. \mathbf{A} is reshaped to a matrix $\mathbf{B} \in \mathbb{R}^{m \times n}$ where the first $m/2$ half rows represent \mathbf{h} and the remaining $m/2$ half rows represent \mathbf{r} . In the convolution layer, a set of 2-dimensional convolutional filters $\Omega = \{\boldsymbol{\omega}_i \mid \boldsymbol{\omega}_i \in \mathbb{R}^{r \times c}\}$ are applied on \mathbf{B} that capture interactions between \mathbf{h} and \mathbf{r} . The resulting feature maps are reshaped and concatenated in order to create a feature vector $\mathbf{v} \in \mathbb{R}^{|\Omega|rc}$. In the next step, \mathbf{v} is mapped into the entity space using a linear transformation $\mathbf{W} \in \mathbb{R}^{|\Omega|rc \times d}$, that is $\mathbf{e}_{h,r} = \mathbf{v}^T \mathbf{W}$. The score for the triple $(h, r, t) \in \mathbb{K}$ is then given by:

$$f(h, r, t) = \mathbf{e}_{h,r} \cdot \mathbf{t}. \quad (34)$$

Since the interaction model can be decomposed into $f(h, r, t) = \langle f'(\mathbf{h}, \mathbf{r}), \mathbf{t} \rangle$, the model is particularly designed to 1-N scoring, i.e. efficient computation of scores for (h, r, t) for fixed h, r and many different t .

t) Relational Graph Convolutional Network: The Relational Graph Convolutional Network (R-GCN) [33] builds on an adapted graph convolutional network (GCN) that can be applied on multi-relational data such as KGs. More concretely, the R-GCN model consists of two major parts: i.) a GCN based entity-encoder that computes latent representations for entities and ii.) an arbitrary interaction model that computes the plausibility of facts. The GCN employed by the entity-encoder is adapted to include typed edges. The forward pass of the GCN is defined by:

$$\mathbf{e}_i^{l+1} = \sigma \left(\sum_{r \in \mathcal{R}} \sum_{j \in \mathcal{N}_i^r} \frac{1}{c_{i,r}} \mathbf{w}_{r,j}^l \mathbf{e}_j^l + \mathbf{w}_0^l \mathbf{e}_i^l \right), \quad (35)$$

where \mathcal{N}_i^r is the set of neighbors of node i that are connected to i by relation r , $c_{i,r}$ is a fixed normalization constant (but it

can also be introduced as an additional parameter), and $\mathbf{W}_r^l \in \mathbb{R}^{d^{(l)} \times d^{(l)}}$ and $\mathbf{W}_0^l \in \mathbb{R}^{d^{(l)} \times d^{(l)}}$ are weight matrices of the l -th layer of the R-GCN. Equation (35) aggregates for each node e_i the latent representations of its neighbors and its own latent representation e_i^l into a new latent representation e_i^{l+1} . In contrast to standard GCNs, R-GCNs define relation specific transformations \mathbf{W}_r^l which depend on the type and direction of an edge. The interaction model computes the plausibility score given the node representations e_i^L that are computed by the last layer L of the R-GCN, i.e., for a given triple $(h, r, t) \in \mathcal{K}$, the corresponding node representations $h := e_i^L$ and $t := e_j^L$ are used:

$$f(h, r, t) = \mathbf{h} \mathbf{R}_r \mathbf{t}, \quad (36)$$

where $\mathbf{R}_r \in \mathbb{R}^{d \times d}$ is a diagonal matrix and $f(h, r, t)$ is the interaction model of DistMult (DistMult was employed in the original work, however, the general approach is not restricted to DistMult). To reduce the number of parameters required for the relation-specific transformation matrices and to avoid over-fitting, two regularization approaches are presented: The first approach (*basis decomposition*), represents the relation-specific transformation matrices as a weighted combination of base matrices, $\{\mathbf{B}_i^l\}_{i=1}^B$, i.e.,

$$\mathbf{W}_r^l = \sum_{b=1}^B \alpha_{rb} \mathbf{B}_i^l. \quad (37)$$

The second approach (*block-diagonal decomposition*), restricts each transformation matrix to a block-diagonal-matrix, i.e.

$$\mathbf{W}_r^l = \text{diag}(\mathbf{B}_{r,1}^l, \dots, \mathbf{B}_{r,B}^l) \quad (38)$$

where $\mathbf{B}_{r,i} \in \mathbb{R}^{(d^{(l)}/B) \times (d^{(l)}/B)}$.

B. Training Approaches

Because most KGs are generated under the open world assumption (OWA), we require training approaches involving techniques such as negative sampling to avoid over-generalization to true facts. Here, we describe two common training approaches found in the literature: the local closed world assumption (LCWA) and the stochastic local closed world assumption (sLCWA). It should be noted that the LCWA and the sLCWA do not affect the evaluation.

1) *Local closed world assumption*: The LCWA was introduced by [29] and used in subsequent works as an approach to generate negative examples during training [32], [24]. In this setting, for any triple $(h, r, t) \in \mathcal{K}$ that has been observed, a set $\mathcal{T}^-(h, r)$ of negative examples is created by considering all triples $(h, r, t_i) \notin \mathcal{K}$ as false. Therefore, for our exemplary KG (Figure 1) for the pair $(\text{Peter}, \text{works_at})$, the triple $(\text{Peter}, \text{works_at}, \text{DHL})$ is a false fact since for this pair only the triple $(\text{Peter}, \text{works_at}, \text{Deutsche Bank})$ is part of the KG. Similarly, we can construct $\mathcal{H}^-(r, t)$ based on all triples $(h_i, r, t) \notin \mathcal{K}$, or $\mathcal{R}^-(h, t)$ based on the triples $(h, r_i, t) \notin \mathcal{K}$. Constructing $\mathcal{R}^-(h, t)$ is a popular choice in visual relation detection domain [34], [35]. However, most of the works in knowledge graph modeling construct only $\mathcal{T}^-(h, r)$ as the set of negative examples, and in the context of this work refer to $\mathcal{T}^-(h, r)$ as the set of negatives examples when speaking about LCWA.

TABLE II
INVESTIGATED INTERACTION MODELS [27] AND THEIR REQUIRED NUMBER OF PARAMETERS. k CORRESPONDS TO THE NUMBER OF NEURONS IN THE HIDDEN LAYER, n_f TO THE NUMBER OF CONVOLUTIONAL KERNELS, k_r AND k_c TO THE HEIGHT AND WIDTH OF THE CONVOLUTIONAL KERNELS.

Model	Parameters
Complex ^a	$ \mathcal{E} 2d + \mathcal{R} 2d$
ConvE ^b	$ \mathcal{E} d + \mathcal{R} d + d + n_f k_r k_c + 2 + 2n_f + 2d + (h - k_r + 1)(w - k_c + 1)n_f d + \mathcal{E} $
ConvKB	$ \mathcal{E} d + \mathcal{R} d + n_f(d + 4) + 1$
DistMult	$ \mathcal{E} d + \mathcal{R} d$
ER-MLP	$ \mathcal{E} d + \mathcal{R} d + k(3d + 2) + 1$
HolE	$ \mathcal{E} d + \mathcal{R} d$
KG2E	$2 \mathcal{E} d + 2 \mathcal{R} d$
NTN	$ \mathcal{E} d + \mathcal{R} k(d^2 + 2d + 2)$
ProjE	$ \mathcal{E} d + \mathcal{R} d + 3d + 1$
R-GCN Basis	$ \mathcal{E} d + (\mathcal{R} + 1)k + kd^2$
R-GCN Block	$ \mathcal{E} d + (\mathcal{R} + 1)d^2/k$
RESCAL	$ \mathcal{E} d + \mathcal{R} d^2$
RotatE ^a	$ \mathcal{E} 2d + \mathcal{R} 2d$
SE	$ \mathcal{E} d + 2 \mathcal{R} d^2$
Simple	$2 \mathcal{E} d + 2 \mathcal{R} d$
TransE	$ \mathcal{E} d + \mathcal{R} d$
TransH	$ \mathcal{E} d + 2 \mathcal{R} d$
TransR	$ \mathcal{E} d_e + \mathcal{R} d_r + d_e d_r$
UM	$ \mathcal{E} d$
TuckER	$ \mathcal{E} d_e + \mathcal{R} d_r + d_e^2 d_r + 4d_e$

^a $2d$, because of complex valued vectors, i.e. imaginary and real part of a number.

^b w and h correspond to the height and weight of the reshaped input.

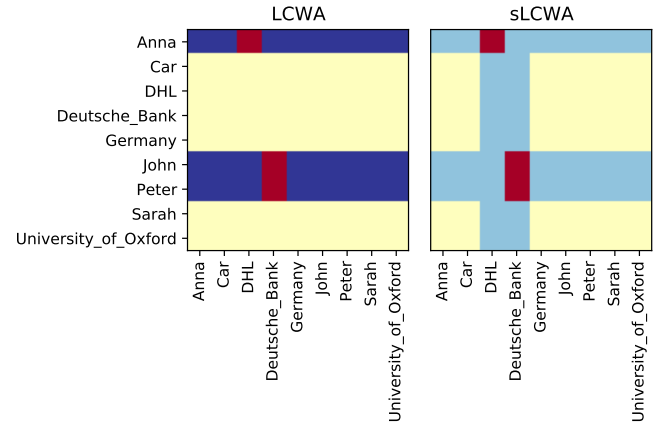


Fig. 3. Visualization of different training approaches for the relation *works_at* in the KG in Figure 1. Red color indicates positive examples, i.e. true triples present in the KG. Dark blue color denotes triples used as negative examples in LCWA. Light blue color sampling candidates for negative examples in sLCWA. Yellow color indicates triples that are not considered.

2) *Stochastic local closed world assumption*: Under the stochastic local closed world assumption (sLCWA), instead of considering all possible triples $(h, r, t_i) \notin \mathcal{K}$, $(h_i, r, t) \notin \mathcal{K}$ or $(h, r_i, t) \notin \mathcal{K}$ as false, we randomly take samples of these sets.

Two common approaches for generating negative samples are uniform negative sampling (UNS) [16] and Bernoulli negative sampling (BNS) [17] in which negative triples are created by corrupting a positive triple $(h, r, t) \in \mathcal{K}$ by replacing either

h or t . We denote with \mathcal{N} the set of all potential negative triples:

$$\mathcal{N} = \bigcup_{(h,r,t) \in \mathcal{K}} \mathcal{N}(h,r,t) \quad (39)$$

$$\mathcal{N}(h,r,t) = \mathcal{T}(h,r) \cup \mathcal{H}(r,t) \quad (40)$$

$$\mathcal{T}(h,r) = \{(h,r,t') \mid t' \in \mathcal{E} \wedge t' \neq t\} \quad (41)$$

$$\mathcal{H}(r,t) = \{(h',r,t) \mid h' \in \mathcal{E} \wedge h' \neq h\} . \quad (42)$$

Theoretically, we would need to exclude all positive triples from this set of candidates for negative triples, i.e., $\mathcal{N}^- = \mathcal{N} \setminus \mathcal{K}$. In practice, however, since usually $|\mathcal{N}| \gg |\mathcal{K}|$, the likelihood of generating a false negative is rather low. Therefore, the additional filter step is often omitted to lower computational cost. It should be taken into account that a corrupted triple that is *not part* of the KG can represent a true fact.

UNS and BNS differ in the way they define sample weights for (h',r,t) or (h,r,t') :

a) **Uniform negative sampling**: With uniform negative sampling (UNS) [16], the first step is to randomly (uniformly) determine whether h or t shall be corrupted for a positive triple $(h,r,t) \in \mathcal{K}$. Afterwards, an entity $e \in \mathcal{E}$ is uniformly sampled and selected as the corrupted head/tail entity.

b) **Bernoulli negative sampling**: With Bernoulli negative sampling (BNS) [17], the probability of corrupting h or t in $(h,r,t) \in \mathcal{K}$ is determined by the property of the relation r : if the relation is a *one-to-many* relation (e.g. *motherOf*), BNS assigns a higher probability to replace h , and if it is a *many-to-one* relation (e.g. *bornIn*) it assigns a higher probability to replace t . More precisely, for each relation $r \in \mathcal{R}$ the average number of tails per head (*tph*) and heads per tail (*hpt*) are first computed. These statistics are then used to define a Bernoulli distribution with parameter $\frac{tph}{tph+hpt}$. For a triple $(h,r,t) \in \mathcal{K}$ the head is corrupted with probability $\frac{tph}{tph+hpt}$ and the tail with probability $\frac{hpt}{tph+hpt}$. The described approach reduces the chance of creating corrupted triples that represent true facts [17].

C. Loss Functions

The loss function can have a significant influence on the performance of KGEMs [7]. In the following, we describe *pointwise*, *pairwise*, and *setwise* loss functions that have been frequently be used within KGEMs. For additional discussion and a slightly different categorization we refer to the work of Mohamed *et al.* [7].

1) **Pointwise Loss Functions**: Let f denote the interaction model of a KGEM. With t_i , we denote a triple (i.e. $t_i \in \mathbb{K}$), and with $l_i \in \{0,1\}$ or $\hat{l}_i \in \{-1,1\}$ its corresponding label, where 1 corresponds to the label of the positive triples, and 0 / -1 to the label of the negative triples. Pointwise loss functions compute an independent loss term for each triple-label pair, i.e. for a batch $B = \{(t_i, l_i)\}_{i=1}^{|B|}$, the loss is given as

$$\mathcal{L} = \frac{1}{|B|} \sum_{(t_i, l_i) \in B} L(t_i, l_i) \quad (43)$$

In the following, we describe four different pointwise losses: The *square error loss*, *binary cross entropy loss (BCEL)*, *pointwise hinge loss*, and *logistic loss*.

a) **Square Error Loss**: The square error loss function computes the squared difference between the predicted scores and the labels $l_i \in \{0,1\}$ [7]:

$$L(t_i, l_i) = \frac{1}{2} (f(t_i) - l_i)^2 \quad (44)$$

The squared error loss strongly penalizes predictions that deviate considerably from the labels, and is usually used for regression problems. For simple models it often permits more efficient optimization algorithms involving analytical solutions of sub-problems, e.g. the Alternating Least Squares algorithm used by [20].

b) **Binary cross entropy loss**: The binary cross entropy loss is defined as [32]:

$$L(t_i, l_i) = -(l_i \cdot \log(\sigma(f(t_i))) + (1 - l_i) \cdot \log(1 - \sigma(f(t_i)))) \quad (45)$$

where $l_i \in \{0,1\}$ and σ represents the logistic sigmoid function. Thus, the problem is framed as a binary classification problem of triples, where the model's outputs are regarded as logits. The loss is not well-suited for translational distance models because these models produce a negative distance as score and cannot produce positive model outputs. ConvE and TuckER were originally trained in a multi-class setting using the binary cross entropy loss where each (h,r) -pair has been classified against $e \in \mathcal{E}$ simultaneously, i.e., if $|\mathcal{E}| = n$, the label vector for each (h,r) -pair has n entries indicating whether the triple (h,r,e_i) is (not) part of the KG, and along each dimension of the label vector a binary classification is performed. It should be noted that there exist different implementation variants of the binary cross entropy loss that address numerical stability. ConvE and TuckER employed a numerically unstable variant, and in the context of this work, we refer to this variant when referring to the binary cross entropy loss.

c) **Pointwise Logistic Loss/Softplus loss**: An alternative, but equivalent formulation of the binary cross entropy loss is the pointwise logistic loss (or Softplus loss (SPL)):

$$L(t_i, l_i) = \log(1 + \exp(-\hat{l}_i \cdot f(t_i))) \quad (46)$$

where $\hat{l}_i \in \{-1,1\}$ [7]. It has been used to train ComplEx, ConvKB, and Simple. We consider both variants separately because both have been used in different model implementations, and their implementation details might yield different results (e.g., to numerical stability).

d) **Pointwise Hinge Loss**: The pointwise hinge loss sets the score of positive examples larger than a margin parameter λ while reducing the scores of negative examples to values below $-\lambda$:

$$L(t_i, l_i) = \max(0, \lambda - \hat{l}_i \cdot f(t_i)) \quad (47)$$

where $\hat{l}_i \in \{-1,1\}$. The loss penalizes scores of positive examples which are smaller than λ , but does not impose any restriction on values $> \lambda$. Similarly, negative scores larger than $-\lambda$ contribute to the loss, whereas all values smaller than $-\lambda$

do not have any loss contribution [7]. Thereby, the model is not encouraged to further optimize triples which are already predicted well enough (according to the margin parameter λ).

2) **Pairwise Loss Functions:** Next, we describe widely applied pairwise loss functions that are used within KGEMs, namely the *pairwise hinge loss* and the *pairwise logistic loss*. They both compare the scores of a positive triple t^+ and a negative triple t^- . The negative triple in a pair is usually obtained by corrupting the positive one. Thus, the pairs often share common head or tail entities and relations. For a batch of pairs $B = \{(t_i^+, t_i^-)\}_{i=1}^{|B|}$, the loss is given as

$$\mathcal{L} = \frac{1}{|B|} \sum_{(t_i^+, t_i^-) \in B} L(f(t_i^-) - f(t_i^+)) . \quad (48)$$

Hence, the loss function evaluates the difference in scores $\Delta = f(t_i^-) - f(t_i^+)$ between a positive and a negative triple, rather than their absolute scores. This is in accordance to the OWA assumption, where we do not assume to have negative labels, but just "less positive" ones.

a) **Pairwise Hinge Loss/Margin ranking loss:** The pairwise hinge loss or margin ranking loss (MRL) is given by

$$L(\Delta) = \max(0, \lambda + \Delta) . \quad (49)$$

b) **Pairwise Logistic Loss:** The pairwise logistic loss is defined as [7]:

$$L(\Delta) = \log(1 + \exp(\Delta)) . \quad (50)$$

Thus, it can be seen as a soft-margin formulation of the pairwise hinge loss with a margin of zero.

3) **Setwise Loss Functions:** Setwise loss functions neither compare individual scores, or pairs of them, but rather more than two triples' scores. Here, we describe the self-adversarial negative sampling loss (NSSAL) and the cross entropy loss (CEL) as examples of such loss functions that has been applied within KGEMs [22], [7].

a) **Self-adversarial negative sampling loss:** Instead of treating each negative sample equally in the loss function, the self-adversarial negative sampling loss (NSSAL) weights negative samples according to the predicted scores by the interaction model [22]. Let $(h, r, t) \in \mathcal{K}$ denote a true triple, and $\{(h'_i, r, t'_i)\}_{i=1}^K$ the set of negative samples generated for it. Then, we define the following distribution over the negative samples

$$p((h'_i, r, t'_i)) = \frac{\exp(\alpha f(h'_i, r, t'_i))}{\sum_{j=1}^K \exp(\alpha f(h'_j, r, t'_j))} , \quad (51)$$

where $\alpha \in \mathbb{R}$ denotes a temperature parameter. The probabilities of the negative triples are then used as weights for them to compute the loss:

$$\mathcal{L} = -\log(\sigma(\gamma + f(h, r, t))) - \sum_{i=1}^K p((h'_i, r, t'_i)) \cdot \log(\sigma(-(\gamma + f(h'_i, r, t'_i)))) . \quad (52)$$

Thus, negative samples for which the model predicts a high score relative to other samples are weighted stronger.

b) **Cross entropy loss:** The cross entropy loss (CEL) has been successfully applied together with 1-N scoring, i.e., predicting for each (h, r) -pair simultaneously a score for each possible tail entity, and framing the problem as a multi-class classification problem [3], [8]. To apply the CEL, first, the labels are normalized in order to form a proper probability distribution. Second, the predicted scores for the tail entities of (h, r) -pair are normalized by a softmax:

$$p(t \mid h, r) = \frac{\exp(f(h, r, t))}{\sum_{t' \in \mathcal{E}} \exp(f(h, r, t'))} . \quad (53)$$

Finally, the cross entropy between the distribution of the normalized scores and the normalized label distribution is computed:

$$\mathcal{L} = - \sum_{t' \in \mathcal{E}} \mathbb{I}[(h, r, t') \in \mathcal{K}] \cdot \log(p(t \mid h, r)) , \quad (54)$$

where \mathbb{I} denotes the indicator function. Note that this loss differs from the multi-class binary cross entropy as it applies a softmax normalization implying that this is a *single-label* multi-class problem.

D. Explicitly Modeling Inverse Relations

Inverse relations introduced by [23] and [36] are explicitly modeled by extending the set of relations \mathcal{R} by a set of inverse relations $r_{inv} \in \mathcal{R}_{inv}$ with $\mathcal{R}_{inv} \cap \mathcal{R} = \emptyset$. This is achieved by training an inverse triple (t, r_{inv}, h) for each triple $(h, r, t) \in \mathcal{K}$. Equipping a KGEM with inverse relations implicitly doubles the relation embedding space of any model that has relation embeddings. The goal is to alter the scoring function, such that the task of predicting the head entities for (r, t) pairs becomes the task of predicting tail entities for (t, r_{inv}) pairs. The explicit training of the implicitly known inverse relations can lead to better model performance [36] and can for some models increase the computational efficiency [32].

IV. EVALUATION METRICS FOR KGEMs

KGEMs are usually evaluated based on link prediction, which is on KG defined as predicting the tail/head entities for $(h, r)/(r, t)$ pairs. For instance, given queries of the form *(Sarah, studied_at, ?)* or *(?, CEO_of, Deutsche Bank)* the capability of a link predictor to predict the correct entities that answer the query, i.e. *(Sarah, studied_at, University of Oxford)* and *(Sarah, CEO_of, Deutsche Bank)* is measured.

However, given the fact that usually true negative examples are not available, both the training and the test set contain only true facts. For this reason, the evaluation procedure is defined as a ranking task in which the capability of the model to differentiate corrupted triples from known true triples is assessed [16]. For each test triple $t^+ = (h, r, t) \in \mathcal{K}_{test}$ two sets of corrupted triples are constructed:

- 1) $\mathcal{H}(r, t) = \{(h', r, t) \mid h' \in \mathcal{E} - \{h\}\}$ which contains all the triples where the head entity has been corrupted, and
- 2) $\mathcal{T}(h, r) = \{(h, r, t') \mid t' \in \mathcal{E} - \{t\}\}$ that contains all the triples with corrupted tail entity.

For each t^+ and its corresponding corrupted triples, the scores are computed and the entities sorted accordingly. Next, the rank of every t^+ among its corrupted triples is determined, i.e. the position in the score-sorted list.

Among the corrupted triples in $\mathcal{H}(r, t) / \mathcal{T}(h, r)$, there might be true triples that are part of the KG. If these false negatives are ranked higher than the current test triple t^+ , the results might get distorted. Therefore, the *filtered* evaluation setting has been proposed [16], in which the corrupted triples are filtered to exclude known true facts from the train and test set. Thus, the rank does not decrease when ranking another true entity higher.

Moreover, we want to draw attention to the fact that the metrics can be further be distorted by *unknown false negatives*, i.e., true triples that are contained in the set of corrupted triples but are not part of the KG (and therefore cannot be filtered out). Therefore, it is essential to investigate the predicted scores of a KGEM and not solely rely on the computed metrics.

Based upon these individual ranks, the following measures are frequently used to summarize the overall performance:

a) **Mean rank**: The mean rank (MR) represents the average rank of the test triples, i.e.

$$\text{MR} = \frac{1}{|\mathcal{K}_{\text{test}}|} \sum_{t \in \mathcal{K}_{\text{test}}} \text{rank}(t) \quad (55)$$

Smaller values indicate better performance.

b) **Adjusted mean rank**: Because the interpretation of the MR depends on the number of available candidate triples, comparing MRs across different datasets (or inclusion of inverse triples) is difficult. This is sometimes further exacerbated in the filtered setting because the number of candidates varies. Therefore, with fewer candidates available, it becomes easier to achieve low ranks. The adjusted mean rank (AMR) [10] compensates for this problem by comparing the mean rank against the expected mean rank under a model with random scores:

$$\text{AMR} = \frac{\text{MR}}{\frac{1}{2} \sum_{t \in \mathcal{K}_{\text{test}}} (\xi(t) + 1)} \quad (56)$$

where $\xi(t)$ denotes the number of candidate triples against which the true triple $t \in \mathcal{K}_{\text{test}}$ is ranked. In the unfiltered setting we have $\xi(t) = |\mathcal{E}| - 1$ for all $t \in \mathcal{K}_{\text{test}}$. Thereby, the measure also adjusts for chance, as a random scoring achieves an expected adjusted mean rank of 1. The AMR has a fixed value range from 0 to 1, where smaller values ($\text{AMR} \ll 1$) indicate better performance.

c) **Mean reciprocal rank**: The mean reciprocal rank (MRR) is defined as:

$$\text{MRR} = \frac{1}{|\mathcal{K}_{\text{test}}|} \sum_{t \in \mathcal{K}_{\text{test}}} \frac{1}{\text{rank}(t)} \quad (57)$$

where $\mathcal{K}_{\text{test}}$ is a set of test triples, i.e. the MRR is the mean over reciprocal individual ranks. However, the MRR is flawed since the reciprocal rank is an ordinal scale and not an interval scale, i.e. computing the arithmetic mean is statistically incorrect [37], [38]. Still, it is often used for early stopping since it is a smooth measure with stronger weight on

small ranks, and less affected by outlier individual ranks than the mean rank. The MRR has a fixed value range from 0 to 1, where larger values indicate better performance.

d) **Hits@K**: Hits@K denotes the ratio of the test triples that have been ranked among the top k triples, i.e.,

$$\text{Hits@k} = \frac{|\{t \in \mathcal{K}_{\text{test}} \mid \text{rank}(t) \leq k\}|}{|\mathcal{K}_{\text{test}}|} \quad (58)$$

Larger values indicate better performance.

e) **Additional Metrics**: Further metrics that might be relevant are the area under the Receiver Operating Characteristic curve (AUC-ROC) and the area under the precision-recall curve (AUC-PR) [11]. However, these metrics require the number of true positives, false positives, true negatives, and false negatives, which in most cases cannot be computed since the KGs are usually incomplete.

V. EXISTING BENCHMARK DATASETS

In this section, we describe the benchmark datasets that have been established to evaluate KGEMs. A summary is also given in Table III.

a) **FB15K**: Freebase is a large cross-domain KG consisting of around 1.2 billion triples and more than 80 million entities. Bordes *et al.* [16] extracted a subset of Freebase, which is used as a benchmark dataset and named it FB15K. It contains 14,951 entities, 1,345 relations, as well as more than half a million triples describing facts about movies, actors, awards, sports, and sports teams [32].

b) **FB15K-237**: FB15K has a test-leakage, i.e. a major part of the test triples ($\sim 81\%$) are inverses of triples contained in the training set: for most of the test triples of the form (h, r, t) , there exists a triple (h, r', t) or (t, r', h) in the training set. Therefore, Toutanova and Chen [39] constructed FB15K-237 in which inverse relations were removed [39]. FB15K-237 contains 14,541 entities and 237 relations.

c) **WN18**: WordNet¹ is a lexical knowledge base in which entities represent terms and are called *synsets*. Relations in WordNet represent conceptual-semantic and lexical relationships (e.g. hyponym). Bordes *et al.* [14] extracted a subset of WordNet named WN18 that is frequently used to evaluate KGEMs. It contains 40,943 synsets and 18 relations.

d) **WN18RR**: Similarly to FB15K, WN18 also has a test-leakage (of approximately 94%) [39]. For instance, for most of the test triples of the form $(h, \text{hyponym}, t)$, there exists a triple $(t, \text{hypernym}, o)$ in the training set. Dettmers *et al.* [32] have shown that a simple rule-based system can obtain results competitive to the state of the art results on WN18. For this reason, they constructed WN18RR by removing inverse relations similarly to the procedure applied to FB15K. WN18RR contains 40,943 entities and 11 relations.

e) **Kinships**: The Kinships [40] dataset describes relationships between members of the Australian tribe *Alyawarra* and consists of 10,686 triples. It contains 104 entities representing members of the tribe and 26 relationship types that represent kinship terms such as *Adiadya* or *Umbaidya* [14]. It is interesting to investigate the model's performance on

¹<https://wordnet.princeton.edu/>

TABLE III
EXISTING BENCHMARK DATASETS.

Dataset	Triples	Entities	Relations
FB15K	592,213	14,951	1,345
FB15K-237	272,115	14,541	237
WN18	151,442	40,943	18
WN18RR	93,003	40,943	11
Kinships	10,686	104	26
Nations	11,191	14	56
UMLS	893,025	135	49
YAGO3-10	1,079,40	132,182	37

Kinships since it is a comparable small KG allowing to perform many hyper-parameter optimization (HPO) iterations for simple and sophisticated interaction models.

f) **Nations**: The Nations [41] dataset contains data about countries and their relationships with other countries. Exemplary relations are *economic_aid* and *accusation* [14].

g) **Unified Medical Language System**: The Unified Medical Language System (UMLS) [42] is an ontology that describes relationships between high-level concepts in the biomedical domain. Examples of contained concepts are *Cell*, *Tissue*, and *Disease*, and exemplary relations are *part_of* and *exhibits* [14], [42].

h) **YAGO3-10**: Yet Another Great Ontology (YAGO) [43] is a KG containing facts that have been extracted from Wikipedia and aligned with WordNet in order to exploit the large amount of information contained in Wikipedia and the taxonomic information included in WordNet. It contains general facts about public figures, geographical entities, movies, and further entities, and it has a taxonomy for those concepts. YAGO3-10 is a subset of YAGO3 [44] (which is an extension of YAGO) that contains entities associated with at least ten different relations. In total, YAGO3-10 has 123,182 entities and 37 relations, and most of the triples describe attributes of persons such as citizenship, gender, and profession [32].

VI. REPRODUCIBILITY STUDIES

The goal of the reproducibility studies was to investigate whether it is possible to replicate experiments based on the information provided in each model’s accompanying paper. If specific information was missing, such as the number of training epochs, we tried to find this information in the accompanying source code if it was accessible. For our study, we focused on the two most frequently used benchmark datasets, FB15K and WN18, as well as their respective subsets FB15K-237 and WN18RR. Table IV illustrates for which models results were reported (in the accompanying publications) for the considered datasets. A checkmark means that results were reported, and green background indicates that the entire experimental setup for the corresponding dataset was described. Results have not been reported for every model for every dataset because some of the benchmark datasets were created after the models were published. Therefore, these models have been excluded from our reproducibility study.

TABLE IV
DENOTES FOR EACH PROPOSED MODEL WHETHER RESULTS HAVE BEEN REPORTED FOR FB15K, WN18, OR THEIR ALTERATIONS. FURTHERMORE, IT INDICATES WHETHER AN OFFICIAL IMPLEMENTATION EXISTS WHERE P CORRESPONDS TO A PYTORCH BASED IMPLEMENTATION, T TO A TENSORFLOW BASED IMPLEMENTATION, AND O TO OTHER IMPLEMENTATIONS. A GREEN BACKGROUND INDICATES THAT THE FULL EXPERIMENTAL SETUP WAS AVAILABLE. THE MODELS HIGHLIGHTED WITH * WHERE INCLUDED IN THE REPRODUCIBILITY STUDY.

Model	Code	FB15K	FB15K-237	WN18	WN18RR
ComplEx*	O	✓		✓	
ConvE*	P	✓	✓	✓	✓
ConvKB	T		✓		✓
DistMult*	-	✓		✓	
ER-MLP	-				
HolE*	O	✓		✓	
KG2E*	-	✓		✓	
NTN	-				
ProjE	T	✓		✓	
RESCAL	O				
R-GCN	-	✓	✓	✓	
RotatE*	P	✓	✓	✓	✓
SE	O				
Simple*	T, P	✓		✓	
TransD*	-	✓		✓	
TransE*	O	✓		✓	
TransH*	-	✓		✓	
TransR*	O	✓		✓	
TuckER*	P	✓	✓	✓	✓
UM	-				

a) **Experimental Setup**: For each KGEM, we applied identical training and evaluation settings as described in their concomitant papers. We ran each experiment four times with random seeds to measure the variance in the obtained results. We evaluated the models based on the ranking metrics MR, AMR, MRR, and Hits@K. As discussed in [4], [10], the exact computation of ranks differs across different codebases, and can lead to significant differences [4]. We follow the nomenclature of Berrendorf *et al.* [10], and report scores based on the optimistic, pessimistic, and realistic rank definitions.

Tables IX, X, IX, and XI represent the results for FB15K, FB15K-237, WN18, and WN18RR where experiments highlighted in blue represent soft-reproducible experiments, i.e., could be reproduced by some margin, and experiments highlighted in orange represent extreme outliers. In the following, we discuss the observations that we made during our experiments.

A. Reproductions Requiring Alternate Hyper-Parameters

One of the observations we made is that for some experiments, results of similar performance could only be obtained based on a different set of hyper-parameter values. For instance, the results for TransE could only be reproduced by adapting the batch size and the number of training epochs. We trained TransE on WN18 for 5000 epochs compared to a reported number of 1000 epochs in order to obtain comparable results. Furthermore, for RotatE on FB15K and WN18, we received better results when adapting the learning rate. The reason for these differences might be explained by the implementation details of the underlying frameworks which have been used to train the models. Authors of early KGEMs

often implemented their training algorithms themselves or used frameworks which were popular at the respective time, but are not used anymore. Therefore, differences between the former and current frameworks may require an adaption of the hyper-parameter values. Even within the same framework, bug fixes or optimizations of the framework can lead to different results based on the used version. Our benchmarking study highlights that with adapted settings, results can be reproduced and even improved.

B. Unreported Hyper-parameters Impedes Reproduction

Some experiments did not report the full setup, which impedes the reproduction of results. For example, the embeddings in the ConvKB experiments have been pre-trained based on TransE. However, the batch size for training TransE has not been reported, which can have a significant effect on the results, as previously discussed. Furthermore, we could not reproduce the results for HoIE on FB15K. The apparent reason is that we could not find the hyper-parameter setting for FB15K, such that we used the same setting as for WN18 which we found in the accompanying implementation.

C. Two Perspectives: Publication versus Implementation

While preparing our experiments, we observed that for some experiments, essential aspects, which are part of the released source code, have not been discussed in the paper. For instance, in the publication describing ConvE, it is not mentioned that inverse triples have been added to the KGs in a pre-processing step. This step seems to be essential to reproduce the results. A second example is SimpleE, for which the predicted scores have been clamped to the range of $[-20, 20]$. This step was not mentioned in the publication, but it can have a significant effect when the model is evaluated based on an optimistic ranking approach, which is the case for SimpleE.

D. Lack of Official Implementations Impedes Reproduction

During our experiments, we observed that for DistMult and TransD, we were able to reproduce the results on WN18, but not on FB15K. A reason might be differences in the implementation details of the frameworks used to train and evaluate the models. For example, the initialization of the embeddings or the normalization of the loss values could have an impact on the performance. Since there exists no official implementation (see Table IV) for DistMult and TransD, it is not possible to check the above-mentioned aspects. Furthermore, we were not able to reproduce the results for TransH for which also no official implementation is available. There exist reference implementations², which slightly differ from the model initially proposed.

E. Reproducibility is Dependent on The Ranking Approach

As discussed in [4], [10], the ranking metrics have been implemented differently by various authors. In our experiments,

we report results based on three common implementations of the ranking metrics: i.) average, ii.) optimistic and iii.) pessimistic ranking (Section IV). If a model predicts the same score for many triples, there will be a large discrepancy between the three ranking approaches. We could observe such a discrepancy for SimpleE for which the results on FB15K (Table XII) and WN18 (Table XIV) were almost 0% based on the average ranking approach, but were much higher based on the optimistic ranking approach. Similar observations for other KGEM have been made in [4].

VII. BENCHMARKING

In our benchmarking studies, we evaluated a large set of different combinations of interaction models, training approaches, loss functions, and the effect of explicitly modeling inverse relations. In particular, we investigated 19 interaction models, two training approaches, and five loss functions on four datasets. We refer to a specific combination of interaction model, training approach, loss function, and whether inverse relations are explicitly modeled as a *configuration*, e.g., RotatE + LCWA + SPL + inverse relations. We do *not* refer to different hyper-parameter values such as batch size or learning rate when we use the term configuration. For each configuration, we used random search to perform the hyper-parameter optimizations over all other hyper-parameters and applied early stopping on the validation set. Each hyper-parameter optimization experiment lasted for a maximum of 24 hours or 100 iterations, in which new hyper-parameters have been sampled in each iteration. Overall, we performed individual hyper-parameter optimizations for more than 1,000 configurations. We retrain the model with the best hyper-parameter setting and report evaluation results on the test set.

Before presenting our results, we provide an overview of the experimental setup, comprising the investigated interaction models, training approaches, loss functions, negative samplers, and datasets. We used the sLCWA and LCWA as training approaches. For the sLCWA we applied a $1:k$ -Scoring as usually done throughout the literature [16], [21], where k denotes the number of negative examples for each positive. For the LCWA, we applied a $1:N$ -Scoring, i.e., we sample each batch against all negatives examples as typically done for training with the LCWA [32]. Table V shows the hyper-parameter ranges for the sLCWA and the LCWA assumptions.

a) Datasets: We performed experiments on the following four datasets: WN18RR, FB15K-237, Kinships and YAGO3-10. We selected WN18RR and FB15K-237 since they are widely applied benchmarking datasets. We chose Kinships and YAGO3-10 to investigate the performance of KGEMs on a small and a larger dataset.

b) Interaction Models: We investigated all interaction models described in Section III-A except R-GCN because its computational requirements impeded an extensive evaluation.

Because of our vast experimental setup and the size of YAGO3-10, we restricted the number of interaction models on YAGO3-10 as otherwise, the computational effort would be prohibitive. Based on their variety of model types as described in Section III-A, we selected the following ten

²<https://github.com/thunlp/OpenKE>

TABLE V
HYPER-PARAMETER RANGES FOR ABLATION EXPERIMENTS

	Hyper-Parameter	Range
Shared	Embedding-Dimension	{64,128,256}
	Initialization	{Xavier}
	Optimizers ^a	{Adam, Adadelta}
	Learning Rate (log scale)	{0.001, 0.1}
	Batch Size ^b	{128, 256, 512}
	Model inverse relations	{Yes, No}
sLCWA	Epochs	1,000
	Loss	{BCEL, MRL, NSSAL, SPL}
	Margin for MRL	{0.5, 1.5, ..., 9.5}
	Margin for NSSAL	{1, 3, 5, ..., 29}
	ADVT for NSSAL	{0.1, 0.2, ..., 1.0}
LCWA	Number of Negatives ^c	{1, 2, ..., 100}
	Loss	{BCEL, CEL, SPL}
	Label Smoothing (log scale)	{0.001, 1.0}

^a For Kinships, we evaluated Adam and Adadelta, and for the remaining datasets we stucked to Adam since it performed almost in every experiment at least equally good as Adadelta and in many experiments significantly better.

^b For YAGO3-10, the batch-size has been sampled from the set {1024, 2048, 2096, 8192}.

^c For YAGO3-10, the number of negative triples per each each positive has been sampled from the set {1, 2, ..., 50}.

interaction models: ComplEx, ConvKB, DistMult, ERMLP, HolE, RESCAL, RotatE, SE, TransD, and TransE.

c) Training Approaches: We trained the interaction models based on the sLCWA (Section III-B2) and the LCWA (Section III-B1) approaches. Due of the extent of our benchmarking study and the fact that YAGO3-10 contains more than 132,000 entities, which makes the training based on the LCWA with 1-n scoring expensive, we restricted the training approach to the sLCWA for YAGO3-10.

d) Loss Functions: We investigated MRL, BCEL, SPL, NSSAL, and CEL since they represent the variety of types described in Section III-C and because they have been previously shown to yield good results. MRL has not been historically used in the 1-N scoring setting likely due to the fact that in 1-N scoring, the number of positive and negative scores in each batch is not known in advance and dynamic. Thus, the number of possible pairs varies as well ranging from $N - 1$ to $(N/2)^2$ for each (h, r) combination. The accompanying variance in memory requirements for each batch thus poses practical challenges. Therefore, we did not use the MRL in combination with the 1-N scoring setting.

e) Negative Sampler: When using the sLCWA, we generated negative samples with UNS. When training with the LCWA and 1-N scoring, no explicit negative sampling was required.

f) Early Stopping: We evaluated each model every 50 epochs and performed early stopping with a patience of 100 epochs on all datasets except for YAGO3-10. There, considering the larger number of triples seen in each epoch we evaluated each model every 10 epochs and performed early stopping with a patience of 50 epochs.

Below, we describe the results of our benchmarking study. In the four following subsections, we summarize the results for each dataset (i.e., Kinships, WN18RR, FB15K-237, YAGO3-

10) along with a discussion of the effect of the models' individual components (i.e., training approaches, loss functions, the explicit modeling of inverse relations) and optimizers on the performance. Finally, we compare the model complexity versus performance. In the appendix, we provide further results. In particular, we provide for each model the results of all tested combinations of interaction model, training approach, and loss function.

A. Results on the Kinships Dataset

Investigating the model performances on Kinships is interesting because it is a comparatively small KG and thus permits for each configuration a large number of HPO iterations for all interaction models. Figure 4 provides a general overview of the results, i.e., performance of the interaction models, loss functions, training approach, the effect modeling inverse relations, and the effect of the optimizers. Overall, several interaction models performed very well (hits@10 higher than 90%), some performed poorly (less than 80% hits@10), and the remaining interaction models revealed average performance (80%-90% hits@10; see Figure 4 as well as Figure 28 and Figure 27 that can be found in the appendix).

The key observations are that the interaction models TransD, TransH, TransR, and UM performed poorly (less than 80%). UM significantly under-performed, which is not surprising since it does not consider the multi-relational information of the data. Overall, for a dataset with similar structural properties such as Kinships, the interaction models ComplEx and Simple seem to be excellent choices since they do not have a very high model complexity, obtain good performances, and are robust throughout a large set of different configurations. In the following, we examine the effect of the single components that define a KGEM.

a) Impact of the Optimizer: On Kinships, we evaluated Adam and Adadelta as optimizers. Our results highlight that in most cases, Adam performs better (in many cases with high margin) or at least equally good as Adadelta (Figure 4). However, ConvE, as one of the few interaction models, performed very well across all configurations that have been trained with Adadelta (Figure 27 in the appendix). In contrast to this, it had issues for some of the configurations that have been trained based on Adam (Figure 28 in the appendix). The worse performing Adam based configurations used the sLCWA as the training approach in combination with inverse relations. Furthermore, KG2E with Adam could only be trained successfully in cases where MRL was used as loss function. For Adadelta, KG2E obtained good results when NSSAL and CEL were used.

Since Adam performed better for the majority of the configurations and the fact that there was always at least one Adam-based configuration that performed equally well as the best Adadelta configuration, we decided to progress only with Adam for the remaining datasets in order to reduce the computational costs.

b) Impact of the Training approach: Figure 5 and Figure 6 depict the effect of the training approaches. The former summarizes the results over the interaction models, and

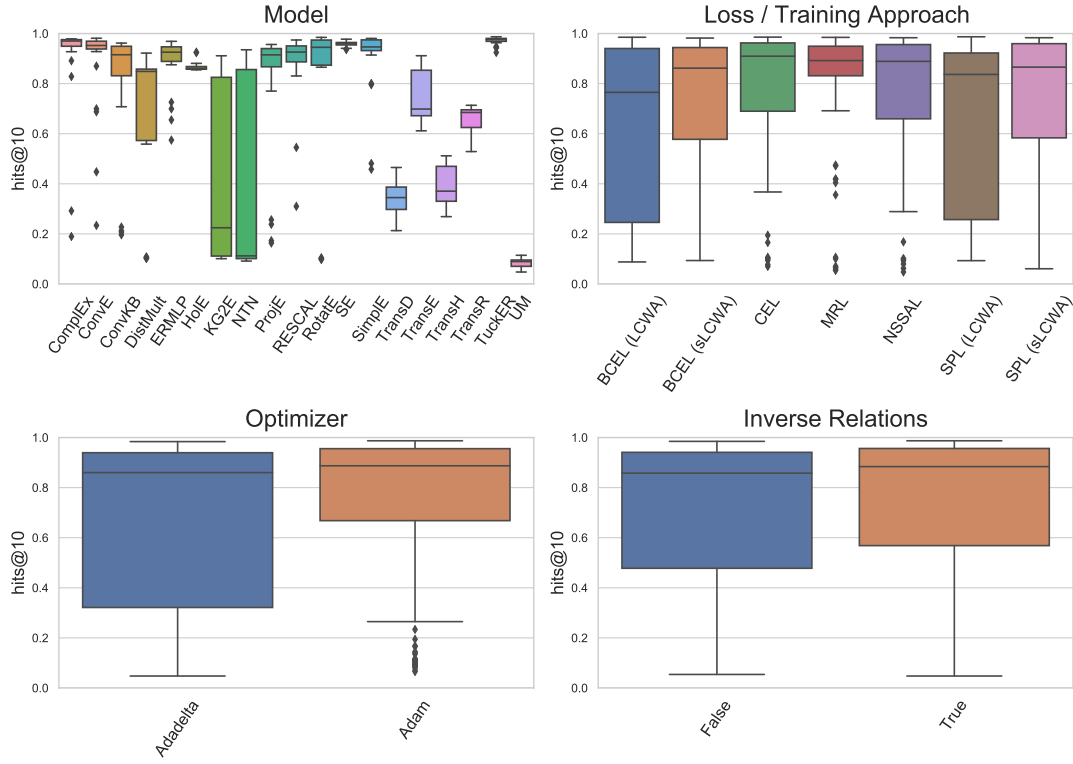


Fig. 4. Overall hits@10 results for Kinships where box-plots summarize the best results across different configurations, i.e., combinations of interaction models, training approaches, loss functions, and the explicit usage of inverse relations.

the latter differentiates between them. At this point, we focus only on the BCEL and the SPL since they have been trained with both training approaches. The key observation is that on Kinships, both training approaches perform comparably well for the BCEL and SPL functions. However, BCEL reveals a slightly less variance when trained in combination with the sLCWA, and the SPL varies less when trained based on the LCWA.

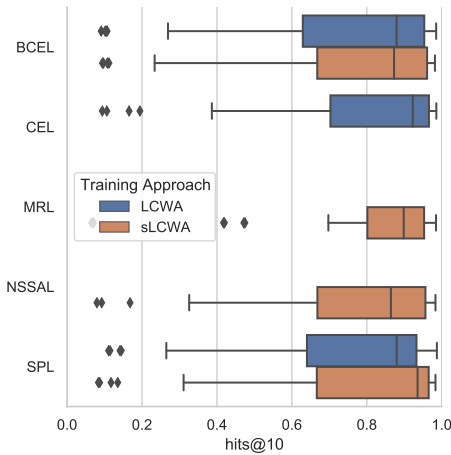


Fig. 5. Impact of the training approach on the performance for a fixed loss function for the Kinships dataset based on Adam.

c) Impact of the Loss Function: Figure 5 highlights that all five loss functions achieve high performance, but at the

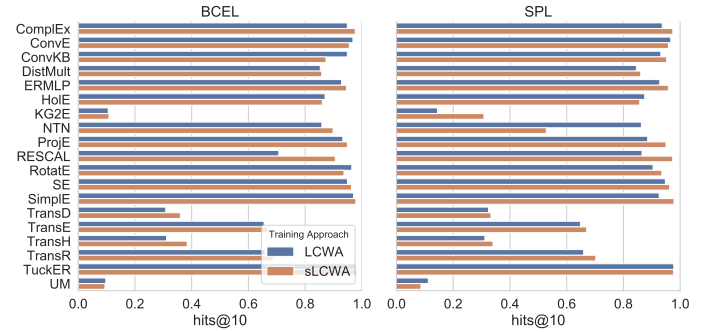


Fig. 6. Impact of training approach on the performance for a fixed interaction model and loss function for the Kinships dataset based on Adam.

same time, most of them exhibit a high variance. An exception is the MRL, which is comparatively robust.

Figure 32 (appendix) reveals that some interaction models (e.g., ComplEx, ConvKB) obtain high results across all loss functions. There are also interaction models that clearly suffer for some of the loss functions (e.g., ConvE suffers from the NSSAL and KG2E performs only well under the MRL).

d) Impact of Explicitly Modeling Inverse Relations:

Figures 7-9 present the effect of explicitly modeling inverse relations. It can be observed that on Kinships, the LCWA benefits from explicit usage of inverse relations (Figure 7).

The loss functions that are trained under the LCWA are more robust when trained with inverse relations. Loss functions that have been trained based on the sLCWA exhibit in

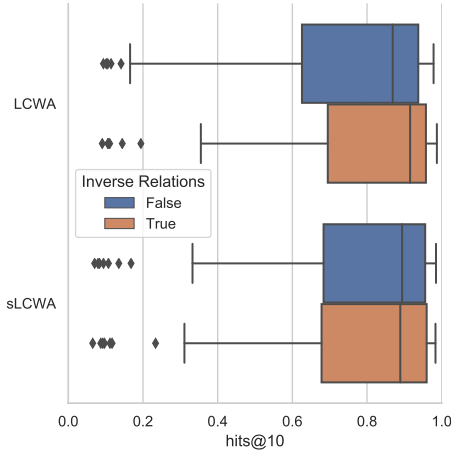


Fig. 7. Impact of explicitly modeling inverse relations on the performance for a fixed training approach for the Kinships dataset based on Adam.

all cases except for NSSAL a lower variance when inverse relations are not explicitly modeled (Figure 8). This observation highlights that the modeling of inverse relations is closely related to the applied training approach.

Considering the interaction models (Figure 9), it can be seen that for some combinations of interaction models and loss functions, the impact of explicitly modeling inverse relations is significant. For instance, when trained based on CEL, ERMLP performs significantly better when trained with explicit inverse relations, whereas ConvE suffers from explicit inverse relations when trained with the MR loss. Here, we want to highlight the close connection to the training approaches. Therefore, it is important to consider these results in the context of the results depicted in Figures 5-7.

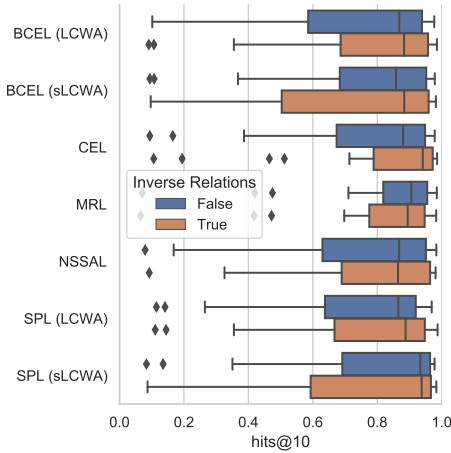


Fig. 8. Impact of explicitly modeling inverse relations on the loss function based on Adam for Kinships.

e) Model Complexity versus Performance: Figure 10 plots the model size against the obtained performance. The results highlight that there is no strong correlation between model size and performance, i.e., models with a small number of parameters can perform equally well as large models on the

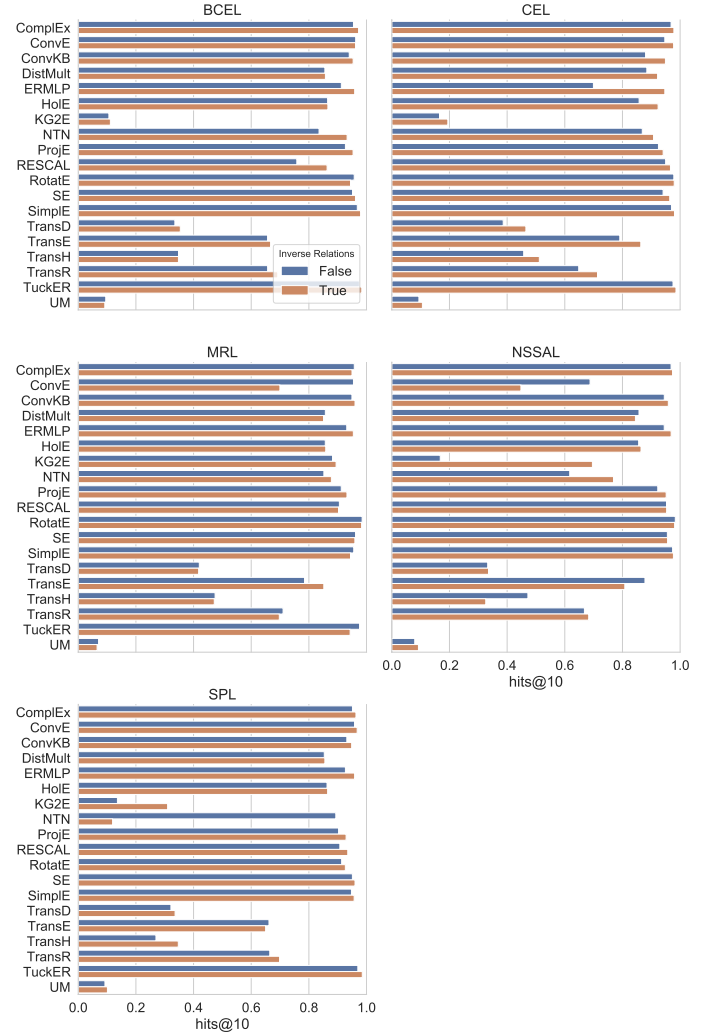


Fig. 9. Impact of explicitly modeling inverse relations on the performance for a fixed interaction model and loss function for the Kinships dataset based on Adam.

Kinships data set. The skyline comprises small UM models, some intermediate HoIE and ProjE models, and larger RotatE and TuckER models. A full list is provided in Table XVIII (in appendix).

B. Results on the WN18RR Dataset

Figure 11 depicts the overall results over WN18RR. A detailed overview over all configurations can be found in Figure 29 in the appendix. The results highlight that there are several combinations of interaction models, loss functions, and training approaches that obtain hits@10 results that are competitive with state of the art results³. In particular, ComplEx (53.14%), ConvE (56.34% compared to 52.00% in the original paper [32]), DistMult (52.70%), ProjE (51.73%), TransE (57.02%), RESCAL (53.64%), RotatE (60.17% compared to 56.61% in the original paper [22]), Simple (50.78%), and TuckER (54.85% compared to 52.6% in the original paper [24]) obtained high performance. Especially the result

³<https://paperswithcode.com/sota/link-prediction-on-wn18rr>

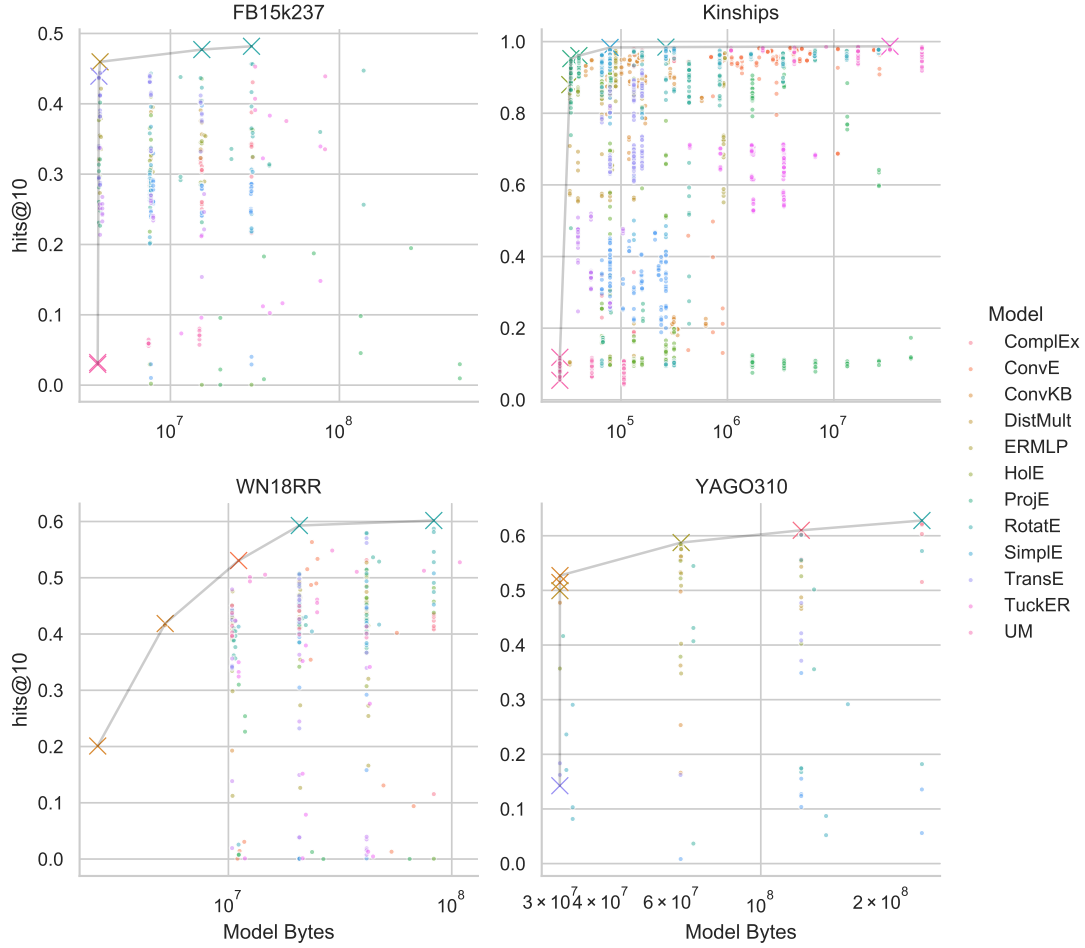


Fig. 10. Scatter plots comparing model size in number of bytes and model performance in terms of Hits@10 for all trained models on each dataset. The color indicates the model type, and the model size is shown on a logarithmic axis. Pareto-optimal models are highlighted by cross symbols. In general we only see a low correlation between model size and performance. A more thorough comparison can be found in Figures 4, 11, 17, and 23.

obtained by TransE is impressive, since it beats most of the published state-of-the-art results. The results highlight that determining an appropriate configuration is fundamental since many many interaction models such as ConvE and TransE reveal a high variance across different configurations. However, with an appropriate configuration, the model complexity can be significantly reduced. For instance, for RotatE, several high performing configurations have been found (Figure 29 in the appendix), and the second-best configuration achieved a hits@10 value of 59.23% (compared to 56.61% in the original paper [22]) while trained with an embedding dimension of 64. RotatE originally has been trained based on the sLCWA and the NSSAL with an embedding dimension of 500 on WN18RR⁴. By changing the training approach from sLCWA to LCWA and changing the loss function from NSSAL to SPL, the embedding dimension could be reduced significantly while getting at the same time an improvement in the hits@10 score. A further interesting observation is the performance of UM, which does not model relations, but can still compete with some of the other interaction models on WN18RR.

This observation might indicate that the relational patterns in WN18RR are not too diverse across relations.

Finally, Figure 11 reveals that we can achieve good performance with all loss functions where BCEL and SPL obtain the best results. However, the loss functions that have been trained in combination with the LCWA express higher variance.

a) Impact of the Training Approach: Figure 12 depicts the impact of the training approach for a fixed loss function. For now, we focus only on BCEL and SPL since they have been trained under both the sLCWA and LCWA. The figure highlights that for both loss functions, the LCWA achieves higher maximum performance, but at the same time, it reveals a larger variance on both loss functions. Consequently, it may be more difficult to find configurations that obtain high performance.

Figure 13 shows the impact of the training approaches for fixed interaction models and used loss functions. The results indicate that for some combinations of interaction models and loss functions, the training approach's choice has a significant impact on the results. For example, RotatE and ConvE show stronger performance when trained with LCWA, whereas TransE and TransH suffer under the LCWA.

⁴https://github.com/DeepGraphLearning/KnowledgeGraphEmbedding/blob/05703200308a1358b9dab9ef1efbf318db22bf44/best_config.sh#L6

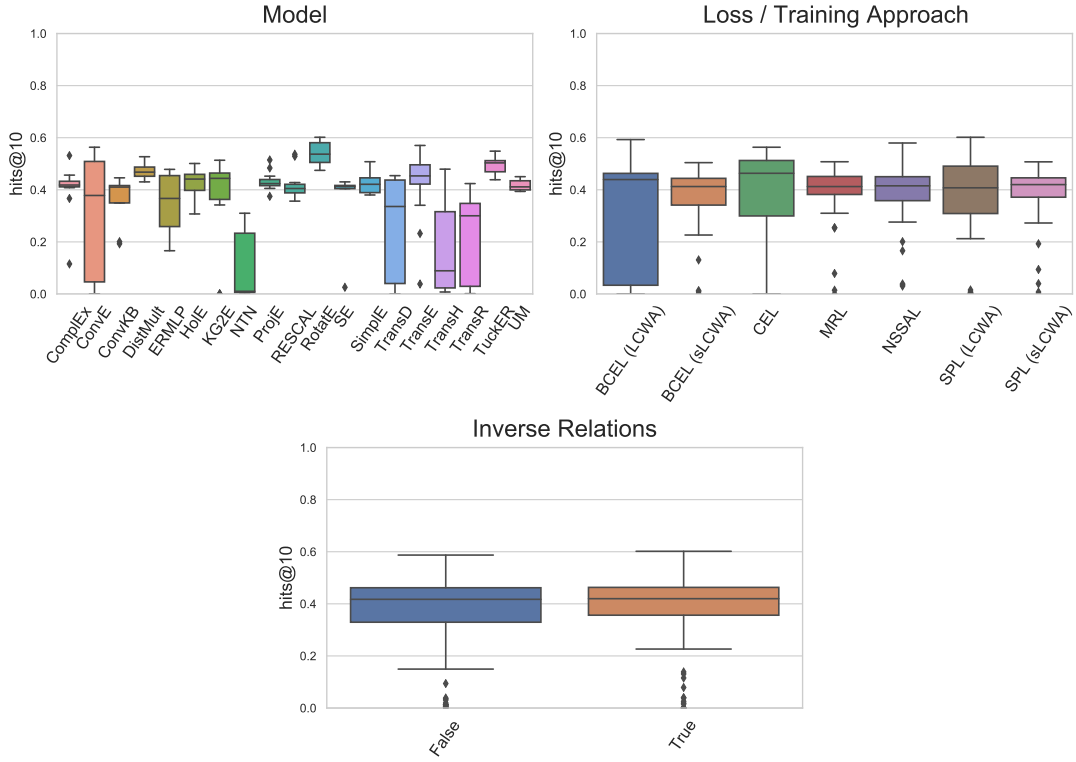


Fig. 11. Overall hits@10 results for WN18RR where box-plots summarize the results across different combinations of interaction models, training approaches, loss functions, and the explicit usage of inverse relations.

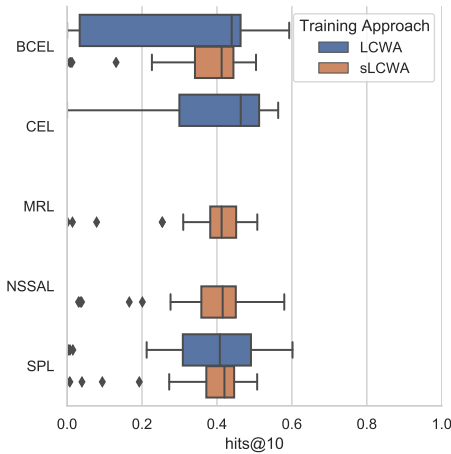


Fig. 12. Impact of the training approach on the performance for a fixed loss function for the WN18RR dataset.

b) Impact of the Loss Function: Figures 11 and 12 depict the performance of the different loss functions. State of the art results for WN18RR are currently between 50% and 60%, and for each loss function, the 50% border could be crossed. The results highlight that there is a trade-off between highest performance and robustness, i.e., SPL and BCEL achieve the highest performance (when trained under the LCWA), but also have high variance (especially BCEL + LCWA).

Figure 33 (appendix) reveals that some interaction models

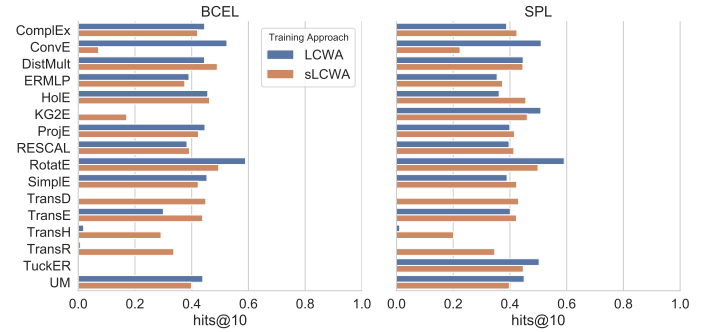


Fig. 13. Impact of training approach on the performance for a fixed interaction model and loss function for the WN18RR dataset.

do not perform well with specific loss functions. For instance, ConvE suffers from the MRL and NSSAL whereas NTN, SE, and TransR suffer from the CEL. However, it should be taken into account that NTN or SE, combined with the CEL, is a computational expensive configuration making extensive HPOs infeasible. Finally, it can be seen that RESCAL benefits from the CEL.

c) Impact of Explicitly Modeling Inverse Relations:

Figure 14 illustrates that the explicit modeling of inverse relations benefits the LCWA. Interestingly, CEL is the only loss function that is trained with the LCWA approach that reveals higher variance when inverse relations are used (Figure 15). BCEL, in combination with the LCWA, is more robust when inverse relations are explicitly modeled. The NSSAL is more

robust when inverse relations are used, but there are only a few high-performing configurations that involve inverse relations. Finally, MRL reveals less variance with inverse relations but does not show any gain in performance.

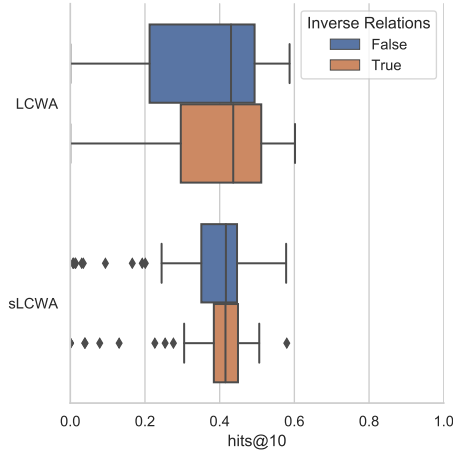


Fig. 14. Impact of explicitly modeling inverse relations on the performance for a fixed training approach for the WN18RR dataset.

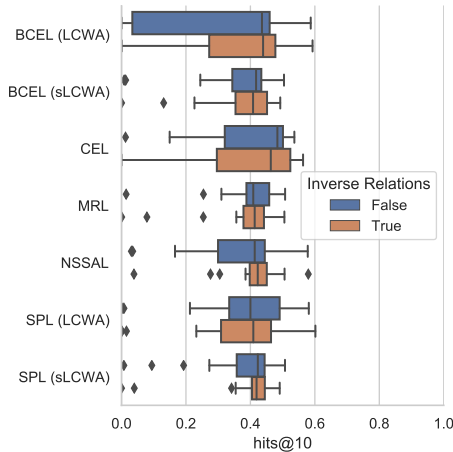


Fig. 15. Impact of explicitly modeling inverse relations on the performance for a fixed loss function for the WN18RR dataset.

d) Model Complexity vs. Performance: Figure 10 highlights that there is no significant correlation between model size and performance. As previously mentioned, we determined a RotatE based configuration that uses an embedding dimension of only 64 that is competitive to the state-of-the-art results that typically use much higher embedding dimensions. The skyline comprises small ConvKB models, an intermediate ConvE model, and large RotatE models. A full list is provided in Table XIX (in appendix).

C. Results on the FB15K-237 Dataset

Figure 17 provides an overall overview of the results obtained on FB15K-237. For the results for each individual configuration, we refer to Figure 30 in the appendix. The results illustrate that the best results of several interaction models such

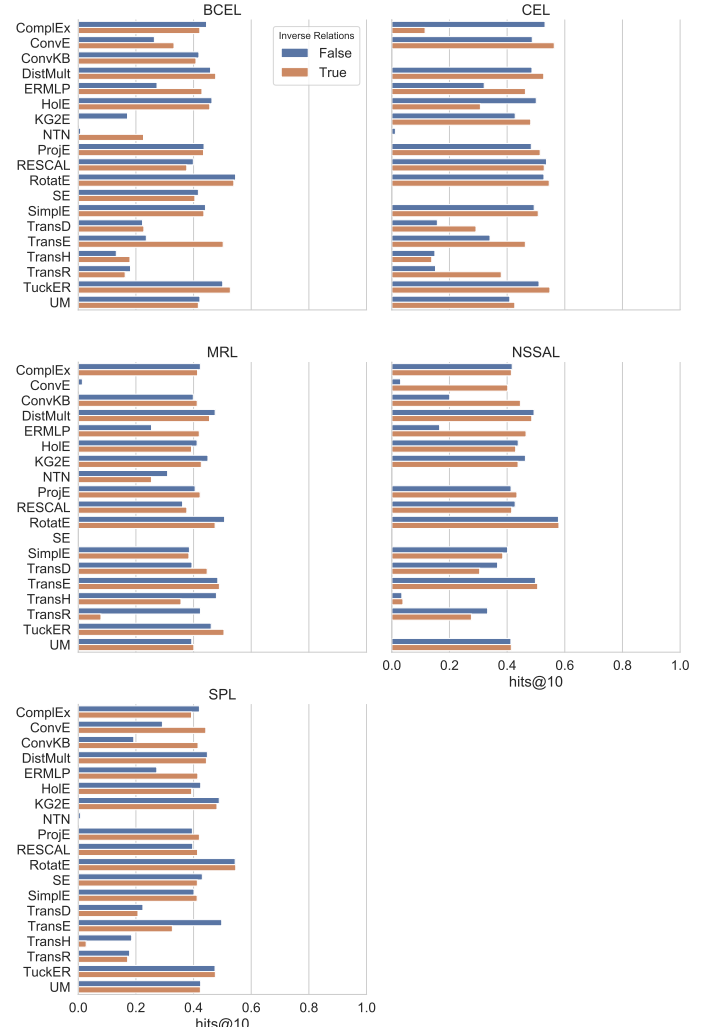


Fig. 16. Impact of explicitly modeling inverse relations on the performance for a fixed interaction model and loss function for the WN18RR dataset.

as DistMult, TransE, RESCAL, and TuckER are comparable, whereas RotatE slightly outperforms the other interaction models. Furthermore, the results show that interaction models such as ProjE, SimpleE, and UM that have been competitive on WN18RR are less competitive on FB15K-237 (at least in our experimental set up). Moreover, the performances of the five loss functions are close to each other.

a) Impact of the Training Approach: Figure 18 shows that for both BCEL and SPL (we focus here only on these two loss functions since they have been trained with both training approaches), the LCWA obtains significantly higher results, but they express a high variance at the same time. Figures 19 and 34 (in the appendix) illustrate that some interaction models benefit from one of the training approaches, whereas others show similar performance with both. For instance, it can be observed that RotatE and TransE perform better in combination with the LCWA approach for both loss functions, whereas ERMLP achieves comparable results for both training approaches.

b) Impact of the Loss Function: Figure 17 illustrates that for all loss functions, comparable results can be achieved,

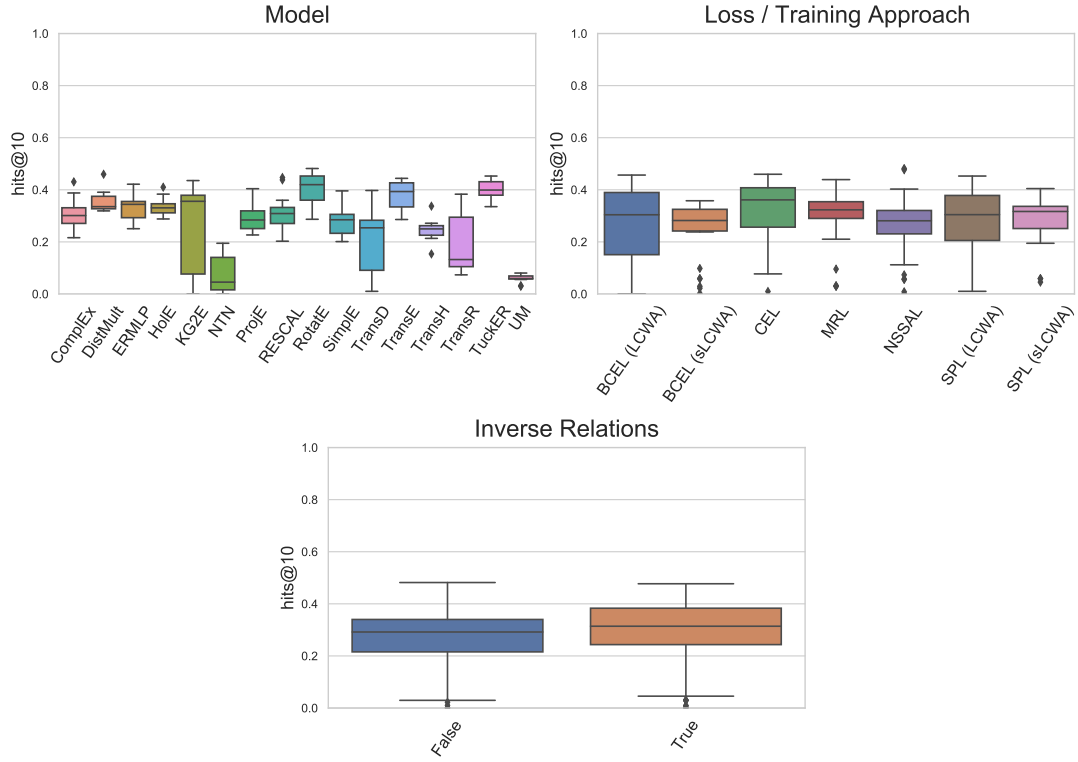


Fig. 17. Overall hits@10 results for FB15K-237 where box-plots summarize the results across different combinations of interaction models, training approaches, loss functions, and the explicit usage of inverse relations.

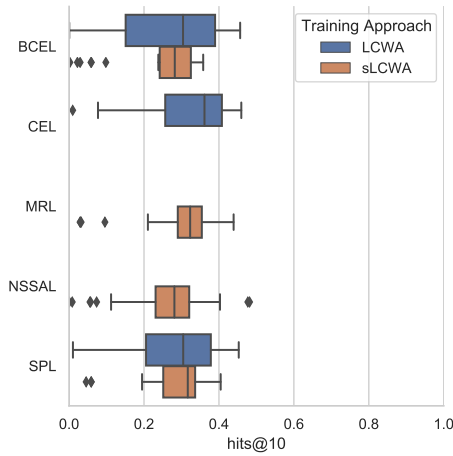


Fig. 18. Impact of the training approach on the performance for a fixed loss function for the FB15K-237 dataset.

but they exhibit higher variance when trained together with the LCWA. However, some interaction models seem to be more sensitive to the usage of the loss function. ComplEx, DistMult, and RESCAL performed better when trained based on the CEL (Figure 34), whereas, TransH, TransR, and TransD benefits from the MRL. Interestingly, all three of them are translational distance models. Finally, BCEL was the only loss function that performed very poorly on KG2E.

c) Impact of Explicitly Modeling Inverse Relations:

Figure 20 reveals as for the previous datasets that the usage

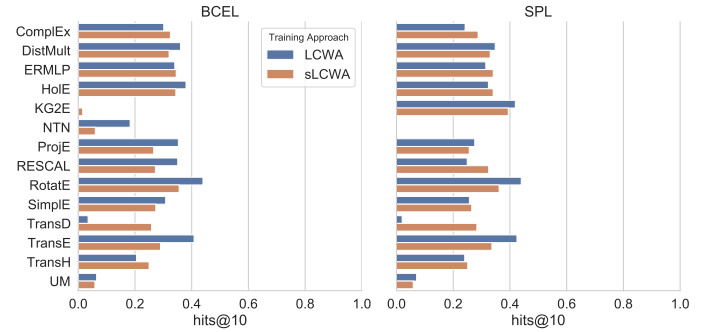


Fig. 19. Impact of training approach on the performance for a fixed interaction model and loss function for the FB15K-237 dataset.

of inverse relations is beneficial for the training based on the LCWA approach. In contrast to the previous datasets, training based on sLCWA leads to higher results while being more robust.

Figure 21 focuses on the effect of explicitly modeling inverse relations for a fixed loss functions. The figure highlights that especially the CEL benefits from explicitly modeling inverse relations, and that the MRL obtains higher results when trained without inverse relations.

Figure 22 depicts the effect of explicitly modeling inverse relations on the combinations of interaction models and loss functions. There are specific combinations of interaction models and loss functions that benefit from the addition of inverse relations. Among those are, for instance, ERMLP, RESCAL,

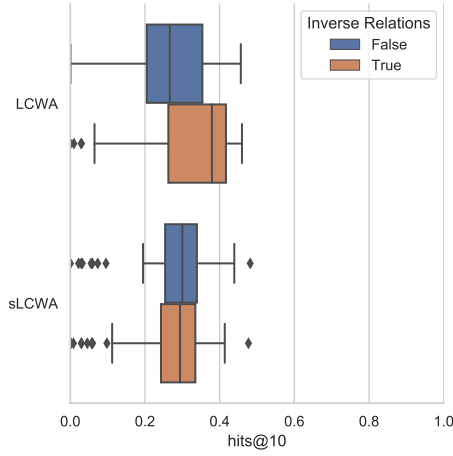


Fig. 20. Impact of explicitly modeling inverse relations on the performance for a fixed training approach for the FB15K-237 dataset.

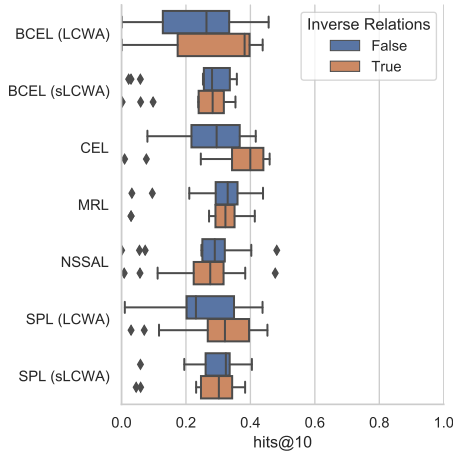


Fig. 21. Impact of explicitly modeling inverse relations on the performance for a fixed loss function for the FB15K-237 dataset.

and TuckER when trained based on BCEL. A second example can be seen for models that have been trained based on SPL for which ComplEx and NTN improve when trained without inverse relations. A very notable observation can be made for CEL: 14 out of 16 interaction models benefit from the addition of inverse relations.

d) Model Complexity vs. Performance: Figure 10 illustrates that for FB15K-237, there is no clear correlation between model size and performance. Tiny models can already obtain similar performance as larger models. The skyline comprises small UM models, some intermediate TransE and DistMult models, and larger RotatE models. A full list is provided in Table XVII (in appendix).

D. Results on the YAGO3-10 Dataset

YAGO3-10 is the largest benchmark dataset in our study. Therefore, it is of interest to investigate how the different interaction models perform on a larger KG. As mentioned in the introduction of this chapter, we reduced the experimental setup for YAGO3-10 in order to reduce the computational

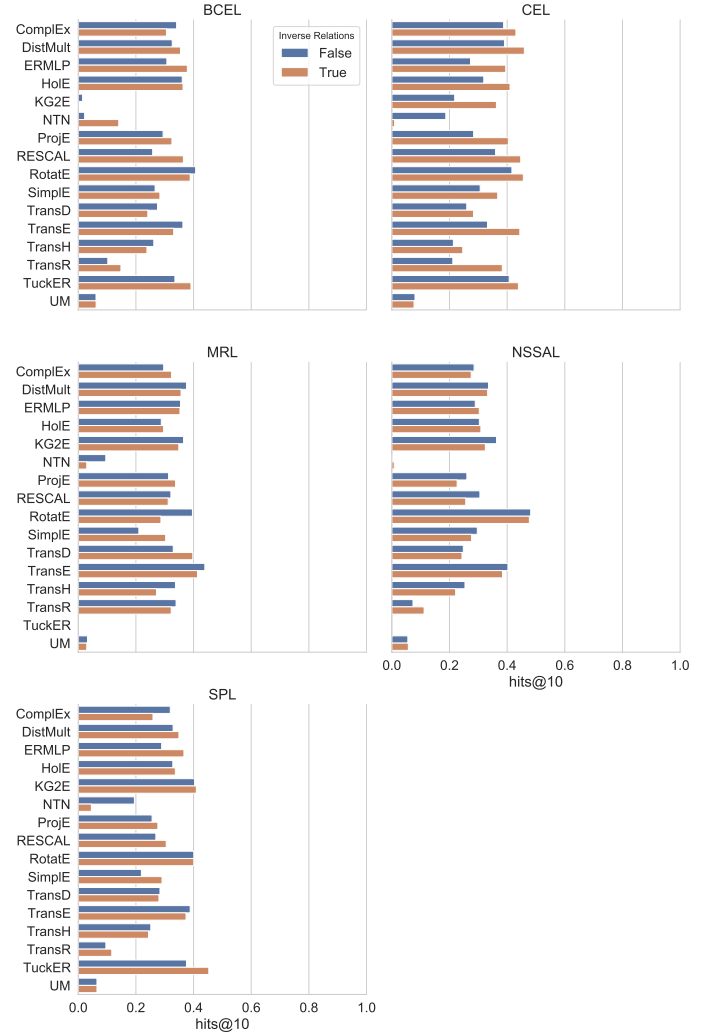


Fig. 22. Impact of explicitly modeling inverse relations on the performance for a fixed interaction model and loss function for the FB15K-237 dataset.

complexity of our entire study. Figure 23 depicts the overall results obtained for YAGO3-10. Detailed results for all configurations are illustrated in Figure 31 in the appendix.

The results highlight the previous observation that the performance of many KGEMs heavily depend on the choice of its components, and is dataset-specific. For instance, RotatE achieves the best performance but also exhibits the largest variance. TransE, which was among the top-performing interaction models on WN18RR, performed poorly on YAGO3-10. One might conclude that TransE performs better on smaller KGs, but the results obtained on Kinships do not support this assumption. It should be taken into account that some interaction models might benefit from the LCWA as observed for TransE on WN18RR. Therefore, TransE might perform much better when trained with the LCWA approach. Remarkably, ComplEx seems to be robust for all sLCWA configurations. With regards to the loss functions, all loss functions except MRL obtain comparable results. Though, the MRL is more robust than other loss functions.

a) Impact of the Loss Function: Figure 24 depicts the impact of the loss functions for fixed interaction models. As

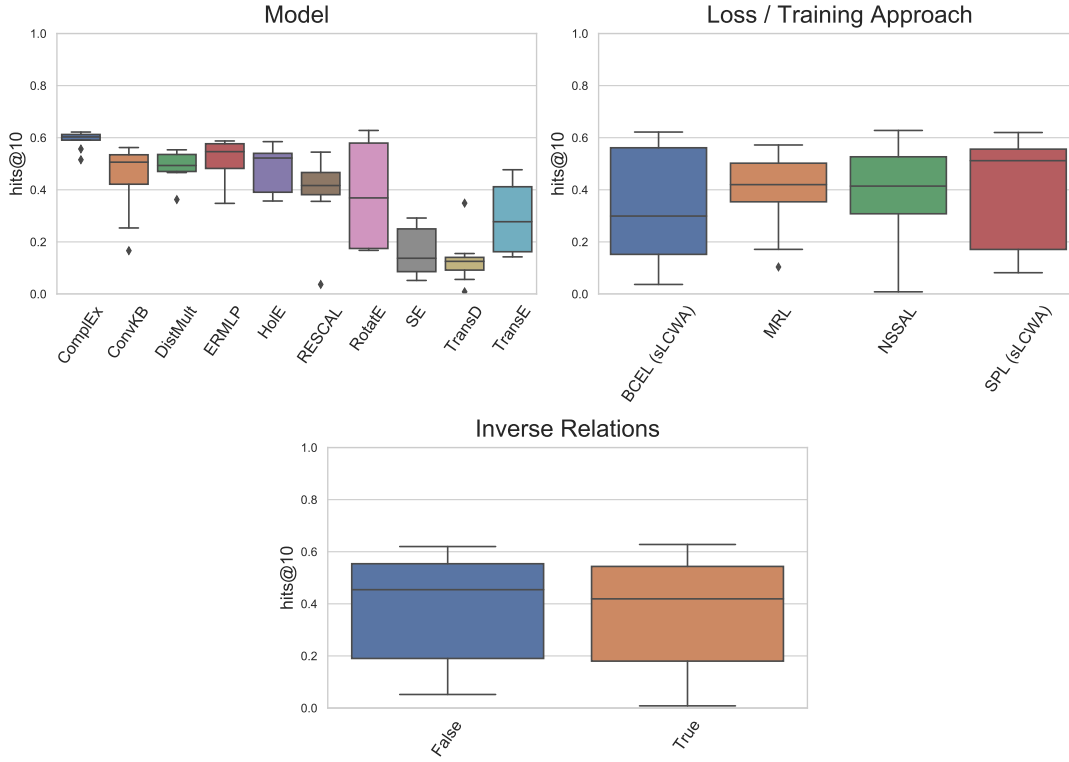


Fig. 23. Overall hits@10 results for YAGO3-10 where box-plots summarize the results across different combinations of interaction models, training approaches, loss functions, and the explicit usage of inverse relations. In contrast, to the previous datasets, the models have only been trained based on the stochastic local closed world assumption.

observed for the previous datasets, some interaction models perform better with specific loss functions. For instance, RotatE and TransE obtain better performance when trained with MRL and NSSAL, whereas ConvKB and RESCAL benefit from SPL.

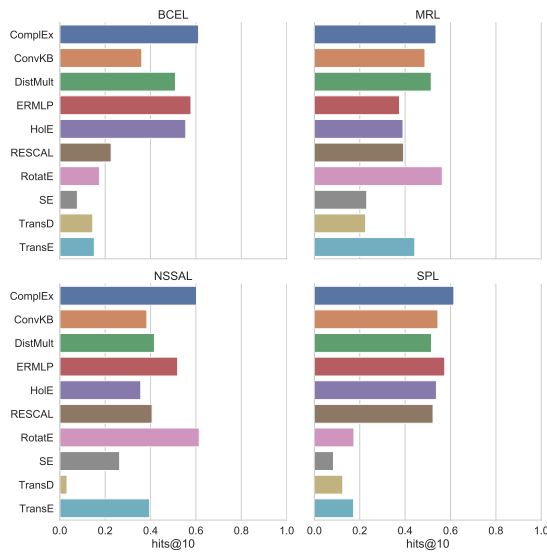


Fig. 24. Impact of the loss functions on the performance for a fixed interaction models for the YAGO3-10 dataset. Because this dataset was only trained under the sLCWA, the boxes are not split like for the other datasets.

b) Impact of Explicitly Modeling Inverse Relations:

Figure 25 shows the effect of explicitly modeling inverse relations for fixed loss functions. Three key aspects can be observed. First, BCEL achieves its best performance when trained with inverse relations. However, the median value is much lower compared to the median obtained by the configurations which do not use inverse relations, indicating that it is more difficult to find an appropriate configuration. Second, MRL is the only loss function for which the addition of inverse relations is beneficial for both performance and robustness. Third, the addition of inverse relations has almost no effect on SPL.

Figure 26 illustrates the effect of the usage of inverse relations on the interaction models. The figure reveals that the combinations of some interaction models and loss functions are not impacted by explicitly modeling inverse relations (e.g., ComplEx and ERMLP for all loss functions except MRL). In contrast, others have clear preferences, e.g., ConvKB suffers from the usage of inverse relations for BCEL and NSSAL and DistMult suffers from inverse relations on BCEL.

c) **Model Complexity vs. Performance:** Figure 10 expresses that there is a low correlation between model size and performance for YAGO3-10. However, the improvement is tiny compared to the differences in model size. It should be taken into account that for KGEMs, the model size is usually dependent on the number of entities and relations. Therefore, dependent on the space complexity of the interaction model (Table II), the size can grow fast for large KGs. The skyline

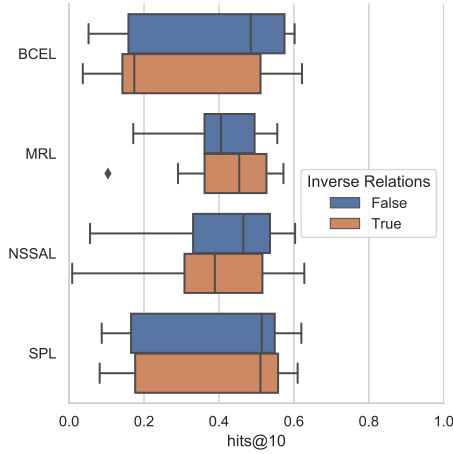


Fig. 25. Impact of explicitly modeling inverse relations on the performance for a fixed loss function for the YAGO3-10 dataset.

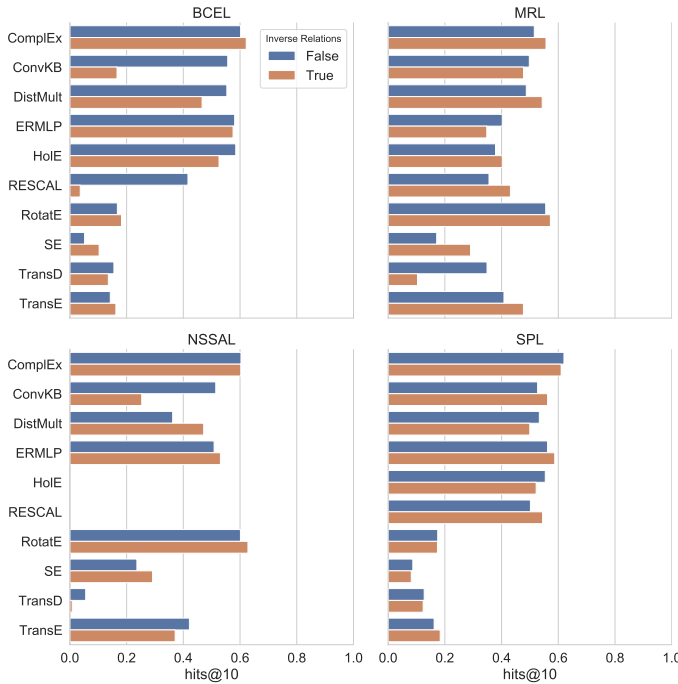


Fig. 26. Impact of explicitly modeling inverse relations on the performance for a fixed interaction model and loss function for the YAGO3-10 dataset.

comprises small TransE, DistMult and ConvKB models, some intermediate ERMLP, and larger ComplEx and RotatE models. A full list is provided in Table XX (in appendix).

VIII. DISCUSSION & FUTURE WORK

Table VI illustrates the extent of our studies and Table VII summarizes the main findings of our work. Although the re-implementation of all machine learning components into a unified, fully configurable framework was a major effort, we believe it is essential to analyze reproducibility and obtain fair results on benchmarking. In particular, we were able to address the issue of incompatible evaluation procedures and preprocessing steps in previous publications that are not obvious.

TABLE VI
EVALUATION STATISTICS

Metric	Value
Datasets	4
Interaction Models	19
Training approaches	2
Loss Functions	5
Negative Samplers	1
Optimizers	2
Ablation Studies	1,035
Number of Experiments	65,301
Compute Time (hours)	21,246

During our reproducibility study, we found that the reproduction of experiments is a major challenge and, in many cases, not possible with the available information in current publications. In particular, we observed the following four main aspects:

- For a set of experiments, the results can sometimes only be reproduced with a different set of hyper-parameter values.
- For some experiments, the entire experimental setup was not provided, impeding the reproduction of experiments.
- The lack of an official implementation hampers the reproduction of results.
- Some results are dependent on the utilized ranking approach (average, optimistic, and pessimistic ranking approach). For example, the optimistic rank may lead to incorrect conclusions about the model's performance.

Our benchmarking study shows that the term KGEM should be used with caution and should be differentiated from the actual interaction model since our results highlight that the specific *combination* of the interaction model, training approach, loss function, and the usage of explicit inverse relations is often fundamental for the performance.

No configuration performs best across all datasets. Depending on the dataset, several configurations can be found that achieve comparable results (Tables XXI-XXIV, and Figures 28-31). Moreover, with an appropriate configuration, the model size can significantly be compressed (see Pareto-optimal configurations in Tables XVII-XX) that has especially a practical relevance when looking for a trade-off between required memory and performance.

The results also highlight that even interaction models such as TransE that have been considered as baselines can outperform state of the art interaction models when trained with an appropriate training approach and loss function. This raises the question of the necessity of the vast number of available interaction models. However, for some interaction models such as RotatE or TuckER, we can observe a good performance across all datasets (note: TuckER has not been evaluated on YAGO3-10, and for WN18RR RotatE outperforms TuckER). For RotatE, we even obtained the state-of-the-art results on WN18RR (similar results were obtained by Graph Attenuated Attention Networks [45]), and for ConvE and TuckER, we obtained results superior to the originally published ones.

TABLE VII
SUMMARY OF MAIN INSIGHTS OVER ALL DATASETS

<i>Interaction Models</i>	
RotatE	Among top-performing interaction models across all datasets.
TuckER	Among top-performing interaction models for Kinships, WN18RR and FB15K-237 (has not been evaluated on YAGO3-10).
TransE	Among top-performing interaction models on WN18RR and FB15K-237.
ComplEx	Among top-performing interaction models on Kinships and YAGO3-10.
ConvE	Among top-performing interaction models on WN18RR (has not been evaluated on FB15K-237 and YAGO3-10).
HolE	Among top-performing interaction models on YAGO3-10.
ERMLP	Among top-performing interaction models on YAGO3-10.
RESCAL	Among top-performing interaction models on FB15K-237.
Simple	Among top-performing interaction models on Kinships.
<i>Loss Functions</i>	
BCEL	Among top-performing loss functions across all datasets.
NSSAL	Among top-performing loss functions across all datasets.
SPL	Among top-performing loss functions across all datasets.
CEL	Among top-performing loss functions on Kinships and FB15K-237 (has not been evaluated on YAGO3-10).
MRL	Among top-performing loss functions on Kinships.
<i>Training Approaches</i>	
sLCWA	Among top-performing training approaches across all datasets.
LCWA	Among top-performing training approaches on Kinships, WN18RR and FB15K-237 (has not been evaluated on YAGO3-10).
<i>Explicit Modeling of Inverse Relations</i>	
	Is usually beneficial in combination with the local closed world assumption.
<i>Configurations</i>	
Performance	Appropriate combination of interaction model, training assumption, loss function, choice of explicitly modeling inverse relations is crucial for the performance, e.g., TransE can compete when with several state-of-the-art interaction models on WN18RR when appropriate configuration is selected. There is no single best configuration that works best for all dataset.
Variance	Some interaction models exhibit a high variance across different configurations, e.g., RotatE on YAGO3-10 (Figure 23)
Pareto-Optimal Configurations	Tables XVII-XX describe Pareto-optimal configurations. It can be seen that there are configurations that require fewer parameters while obtaining almost the same performance. In some cases, for the same interaction model, the model can be significantly compressed.
<i>Reproducibility</i>	
Results	For FB15K, two out of 12, for WN18, six out of 12, for FB15K-237, one out of three, and for WN18RR, two out of three experiments can be categorized as soft-reproducible.
Code	For four out of 13 models, no official implementation was available.
Parameters	For four out of 13 paper, source code was available and full experimental setup was precisely described.
<i>General Insights</i>	
SOTA	For WN18RR, we achieve based on a RotatE-configuration (together with Graph Attenuated Attention Networks [45]) state-of-the-art results in terms of hits@10 through our study (60.17% Hits@10). Furthermore, we found a TransE configuration that achieves high performance beating most of the published SOTA results (57.02% Hits@10). Based on our results, we emphasize to further investigate the hyper-parameters space for the most promising configurations for the remaining benchmarking datasets.
Improvements	For ConvE (56.34% compared to 52.00% [32]) and TuckER (54.85% compared to 52.6% [24]), we are beating the reported results in the original papers due selecting appropriate configurations and hyper-parameters on WN18RR.

ComplEx proved to be a very robust interaction model across different configurations. This can, in particular, be observed from the results obtained on YAGO3-10 (Figure 23).

We discovered that no loss function consistently achieves the best results. Instead it can be seen that with different loss functions such as the BCEL, NSSAL, and SPL good results can be obtained across all datasets. Remarkably, the MRL is overall the worst-performing loss function — it is only among the top-performing loss functions for Kinships. However, one might argue that the MRL is the most compatible loss function with the sLCWA since it does not assume artificially generated negative examples to be actually false in contrast to the other loss functions used. The MRL only learns to score positive examples higher than *corresponding* negative examples. However, it does not ensure that a negative example is scored lower than every other positive example. Thus, the

absolute score values are not interpretable and cannot be used to compared triples without common head/tail entities. They can only be interpreted relatively, and only when comparing scores for triples with the same $(hr)/(rt)$. Although loss functions such as BCEL or SPL treat generated negative triples as true negatives that actually contain also unknown positive examples, they obtain good performance. This might be explained by the fact that usually the set of unknown triples are dominated by false triples. Therefore, it is likely that a major part of the generated triples are actually negative. Consequently, the KGEM learns to distinguish better positive from negative examples.

Considering the explicit usage of inverse relations, we found out that the impact of inverse relations can be significant, especially when the interaction model is trained under the LCWA. This might be explained by the fact that based on

the LCWA-training, the KGEM only learns to perform *one-side predictions* (i.e., it learns to either predict head or tail entities), but during the evaluation, it is asked to perform *both-side predictions*. Through the inclusion of inverse relations, the model learns to perform both-side predictions based on one side, i.e., $(*, r, t)$ can be predicted through $(t, r_{inverse}, *)$. Overall, our results indicate that further investigations on FB15K-237 and YAGO3-10 might lead to results that are competitive to the state-of-the-art.

Looking forwards, it would be of great interest to re-investigate previously performed studies that analyze the relationship between the performance of KGEMs and the properties of the underlying KGs to verify that their findings indeed can be attributed to the *interaction model* alone, rather than the exact configuration including the loss function, the training assumption and the explicit modeling of inverse triples. Further, the effect of explicitly modeling inverse relations has not been analyzed in depth, in particular how the learned representations of a relation and its inverse are related to each other. Ultimately, we believe our work provides an empirical foundation for such studies and a practical tool to execute them.

ACKNOWLEDGMENT

We want to thank the Center for Information Services and High Performance Computing (ZIH) at TU Dresden for generous allocations of computer time and the Technical University of Denmark for providing us access to their DTU Compute GPU cluster that enabled us to conduct our studies. This work was funded by the German Federal Ministry of Education and Research (BMBF) under Grant No. 01IS18036A and Grant No. 01IS18050D (project MLWin) as well as the Innovation Fund Denmark with the Danish Center for Big Data Analytics driven Innovation (DABAI).

REFERENCES

- [1] Q. Wang, Z. Mao, B. Wang, and L. Guo, "Knowledge graph embedding: A survey of approaches and applications," *IEEE Transactions on Knowledge and Data Engineering*, vol. 29, no. 12, pp. 2724–2743, 2017.
- [2] F. Akrami, L. Guo, W. Hu, and C. Li, "Re-evaluating embedding-based knowledge graph completion methods," in *Proceedings of the 27th ACM International Conference on Information and Knowledge Management*. ACM, 2018, pp. 1779–1782.
- [3] R. Kadlec, O. Bajgar, and J. Kleindienst, "Knowledge base completion: Baselines strike back," *arXiv preprint arXiv:1705.10744*, 2017.
- [4] Z. Sun, S. Vashishth, S. Sanyal, P. Talukdar, and Y. Yang, "A re-evaluation of knowledge graph completion methods," *arXiv preprint arXiv:1911.03903*, 2019.
- [5] B. Yang, W. Yih, X. He, J. Gao, and L. Deng, "Embedding entities and relations for learning and inference in knowledge bases," in *3rd International Conference on Learning Representations, ICLR 2015, San Diego, CA, USA, May 7-9, 2015, Conference Track Proceedings*, 2015. [Online]. Available: <http://arxiv.org/abs/1412.6575>
- [6] F. Akrami, M. S. Saef, Q. Zhang, W. Hu, and C. Li, "Realistic re-evaluation of knowledge graph completion methods: An experimental study," in *Proceedings of the 2020 ACM SIGMOD International Conference on Management of Data*, 2020, pp. 1995–2010.
- [7] S. K. Mohamed, V. Nováček, P.-Y. Vandenbussche, and E. Muñoz, "Loss functions in knowledge graph embedding models," in *DL4KG@ ESWC*. CEUR-WS. org, 2019, vol. 2377, pp. 1–10.
- [8] D. Ruffinelli, S. Broscheit, and R. Gemulla, "You {can} teach an old dog new tricks! on training knowledge graph embeddings," in *International Conference on Learning Representations*, 2020.
- [9] A. Rossi, D. Firmani, A. Matinata, P. Merialdo, and D. Barbosa, "Knowledge graph embedding for link prediction: A comparative analysis," *arXiv preprint arXiv:2002.00819*, 2020.
- [10] M. Berrendorf, E. Faerman, L. Vermue, and V. Tresp, "Interpretable and fair comparison of link prediction or entity alignment methods with adjusted mean rank," *arXiv preprint arXiv:2002.06914*, 2020.
- [11] M. Nickel, K. Murphy, V. Tresp, and E. Gabrilovich, "A review of relational machine learning for knowledge graphs," *Proceedings of the IEEE*, vol. 104, no. 1, pp. 11–33, 2015.
- [12] B. Köttnis and V. Nastase, "Analysis of the impact of negative sampling on link prediction in knowledge graphs," *arXiv preprint arXiv:1708.06816*, 2017.
- [13] L. A. Galárraga, C. Teflioudi, K. Hose, and F. Suchanek, "Amie: association rule mining under incomplete evidence in ontological knowledge bases," in *Proceedings of the 22nd international conference on World Wide Web*, 2013, pp. 413–422.
- [14] A. Bordes, X. Glorot, J. Weston, and Y. Bengio, "A semantic matching energy function for learning with multi-relational data," *Machine Learning*, vol. 94, no. 2, pp. 233–259, 2014.
- [15] A. Bordes, J. Weston, R. Collobert, and Y. Bengio, "Learning structured embeddings of knowledge bases," in *Proceedings of the Twenty-Fifth AAAI Conference on Artificial Intelligence, AAAI 2011, San Francisco, California, USA, August 7-11, 2011*, 2011. [Online]. Available: <http://www.aaai.org/ocs/index.php/AAAI/AAAI11/paper/view/3659>
- [16] A. Bordes, N. Usunier, A. García-Durán, J. Weston, and O. Yakhnenko, "Translating embeddings for modeling multi-relational data," in *Advances in Neural Information Processing Systems 26: 27th Annual Conference on Neural Information Processing Systems 2013. Proceedings of a meeting held December 5-8, 2013, Lake Tahoe, Nevada, United States.*, 2013, pp. 2787–2795. [Online]. Available: <http://papers.nips.cc/paper/5071-translating-embeddings-for-modeling-multi-relational-data>
- [17] Z. Wang, J. Zhang, J. Feng, and Z. Chen, "Knowledge graph embedding by translating on hyperplanes," in *Proceedings of the Twenty-Eighth AAAI Conference on Artificial Intelligence, July 27 - 31, 2014, Québec City, Québec, Canada.*, 2014, pp. 1112–1119. [Online]. Available: <http://www.aaai.org/ocs/index.php/AAAI/AAAI14/paper/view/8531>
- [18] Y. Lin, Z. Liu, M. Sun, Y. Liu, and X. Zhu, "Learning entity and relation embeddings for knowledge graph completion," in *Proceedings of the Twenty-Ninth AAAI Conference on Artificial Intelligence, January 25-30, 2015, Austin, Texas, USA.*, 2015, pp. 2181–2187. [Online]. Available: <http://www.aaai.org/ocs/index.php/AAAI/AAAI15/paper/view/9571>
- [19] G. Ji, S. He, L. Xu, K. Liu, and J. Zhao, "Knowledge graph embedding via dynamic mapping matrix," in *Proceedings of the 53rd Annual Meeting of the Association for Computational Linguistics and the 7th International Joint Conference on Natural Language Processing of the Asian Federation of Natural Language Processing, ACL 2015, July 26-31, 2015, Beijing, China, Volume 1: Long Papers*, 2015, pp. 687–696. [Online]. Available: <http://aclweb.org/anthology/P/P15/P15-1067.pdf>
- [20] M. Nickel, V. Tresp, and H. Krieger, "A three-way model for collective learning on multi-relational data," in *Proceedings of the 28th International Conference on Machine Learning, ICML 2011, Bellevue, Washington, USA, June 28 - July 2, 2011*, 2011, pp. 809–816. [Online]. Available: https://icml.cc/2011/papers/438_icmlpaper.pdf
- [21] T. Trouillon, J. Welbl, S. Riedel, É. Gaussier, and G. Bouchard, "Complex embeddings for simple link prediction," in *Proceedings of the 33rd International Conference on Machine Learning, ICML 2016, New York City, NY, USA, June 19-24, 2016*, 2016, pp. 2071–2080.
- [22] Z. Sun, Z. Deng, J. Nie, and J. Tang, "Rotate: Knowledge graph embedding by relational rotation in complex space," *CoRR*, vol. abs/1902.10197, 2019. [Online]. Available: <http://arxiv.org/abs/1902.10197>
- [23] S. M. Kazemi and D. Poole, "Simple embedding for link prediction in knowledge graphs," in *Advances in Neural Information Processing Systems*, 2018, pp. 4284–4295.
- [24] I. Balazević, C. Allen, and T. M. Hospedales, "Tucker: Tensor factorization for knowledge graph completion," *arXiv preprint arXiv:1901.09590*, 2019.
- [25] L. R. Tucker *et al.*, "The extension of factor analysis to three-dimensional matrices," *Contributions to mathematical psychology*, vol. 110119, 1964.
- [26] B. Shi and T. Wenginger, "Proje: Embedding projection for knowledge graph completion," in *Thirty-First AAAI Conference on Artificial Intelligence*, 2017.
- [27] M. Nickel, L. Rosasco, and T. A. Poggio, "Holographic embeddings of knowledge graphs," in *Proceedings of the Thirtieth AAAI Conference on Artificial Intelligence, February 12-17, 2016, Phoenix*,

- Arizona, USA., 2016, pp. 1955–1961. [Online]. Available: <http://www.aaai.org/ocs/index.php/AAAI/AAAI16/paper/view/12484>
- [28] S. He, K. Liu, G. Ji, and J. Zhao, “Learning to represent knowledge graphs with gaussian embedding,” in *Proceedings of the 24th ACM International on Conference on Information and Knowledge Management*. ACM, 2015, pp. 623–632.
- [29] X. Dong, E. Gabrilovich, G. Heitz, W. Horn, N. Lao, K. Murphy, T. Strohmann, S. Sun, and W. Zhang, “Knowledge vault: a web-scale approach to probabilistic knowledge fusion,” in *The 20th ACM SIGKDD International Conference on Knowledge Discovery and Data Mining, KDD '14, New York, NY, USA - August 24 - 27, 2014*, 2014, pp. 601–610. [Online]. Available: <https://doi.org/10.1145/2623330.2623623>
- [30] R. Socher, D. Chen, C. D. Manning, and A. Ng, “Reasoning with neural tensor networks for knowledge base completion,” in *Advances in neural information processing systems*, 2013, pp. 926–934.
- [31] D. Q. Nguyen, T. D. Nguyen, D. Q. Nguyen, and D. Phung, “A novel embedding model for knowledge base completion based on convolutional neural network,” *arXiv preprint arXiv:1712.02121*, 2017.
- [32] T. Dettmers, P. Minervini, P. Stenetorp, and S. Riedel, “Convolutional 2d knowledge graph embeddings,” in *Proceedings of the Thirty-Second AAAI Conference on Artificial Intelligence, (AAAI-18), the 30th innovative Applications of Artificial Intelligence (IAAI-18), and the 8th AAAI Symposium on Educational Advances in Artificial Intelligence (EAAI-18), New Orleans, Louisiana, USA, February 2-7, 2018*, 2018, pp. 1811–1818. [Online]. Available: <https://www.aaai.org/ocs/index.php/AAAI/AAAI18/paper/view/17366>
- [33] M. S. Schlichtkrull, T. N. Kipf, P. Bloem, R. van den Berg, I. Titov, and M. Welling, “Modeling relational data with graph convolutional networks,” in *The Semantic Web - 15th International Conference, ESWC 2018, Heraklion, Crete, Greece, June 3-7, 2018, Proceedings*, 2018, pp. 593–607. [Online]. Available: https://doi.org/10.1007/978-3-319-93417-4_38
- [34] H. Zhang, Z. Kyaw, S.-F. Chang, and T.-S. Chua, “Visual translation embedding network for visual relation detection,” in *Proceedings of the IEEE conference on computer vision and pattern recognition*, 2017, pp. 5532–5540.
- [35] S. Sharifzadeh, S. M. Baharlou, M. Berrendorf, R. Koner, and V. Tresp, “Improving visual relation detection using depth maps,” in *2020 25th International Conference on Pattern Recognition (ICPR)*. IEEE, 2020.
- [36] T. Lacroix, N. Usunier, and G. Obozinski, “Canonical tensor decomposition for knowledge base completion,” *arXiv preprint arXiv:1806.07297*, 2018.
- [37] N. Fuhr, “Some common mistakes in ir evaluation, and how they can be avoided,” *SIGIR Forum*, vol. 51, no. 3, pp. 32–41, Feb. 2018. [Online]. Available: <http://doi.acm.org/10.1145/3190580.3190586>
- [38] S. S. Stevens et al., “On the theory of scales of measurement,” 1946.
- [39] K. Toutanova and D. Chen, “Observed versus latent features for knowledge base and text inference,” in *Proceedings of the 3rd Workshop on Continuous Vector Space Models and their Compositionality*, 2015, pp. 57–66.
- [40] W. W. Denham, “The detection of patterns in alyawara nonverbal behavior,” Ph.D. dissertation, University of Washington, Seattle., 1973.
- [41] R. J. Rummel, *The dimensionality of nations project: attributes of nations and behavior of nations dyads, 1950-1965*. Inter-university Consortium for Political Research, 1976, no. 5409.
- [42] A. T. McCray, “An upper-level ontology for the biomedical domain,” *International Journal of Genomics*, vol. 4, no. 1, pp. 80–84, 2003.
- [43] T. Rebele, F. Suchanek, J. Hoffart, J. Biega, E. Kuzey, and G. Weikum, “Yago: A multilingual knowledge base from wikipedia, wordnet, and geonames,” in *International Semantic Web Conference*. Springer, 2016, pp. 177–185.
- [44] F. Mahdisoltani, J. Biega, and F. M. Suchanek, “Yago3: A knowledge base from multilingual wikipedias,” 2013.
- [45] R. Wang, B. Li, S. Hu, W. Du, and M. Zhang, “Knowledge graph embedding via graph attenuated attention networks,” *IEEE Access*, 2019.

APPENDIX

ADDITIONAL RESULTS FROM REPRODUCIBILITY STUDY

TABLE VIII

REPRODUCTION OF STUDIES ON FB15K WITHOUT INDICATING THE STANDARD DEVIATION WHERE **PUB** REFERS TO PUBLISHED RESULTS, **R** TO RESULTS BASED ON THE REALISTIC RANKING, **O** TO RESULTS BASED ON THE OPTIMISTIC RANKING, AND **P** TO RESULTS BASED ON THE PESSIMISTIC RANKING. WE ONLY SHOW THE RESULTS OF THE OPTIMISTIC AND PESSIMISTIC RANKING IN CASE THEY DIFFER FROM THE REALISTIC RANKING. MODELS HIGHLIGHTED IN **BLUE** INDICATE THE EXPERIMENTS ARE SOFT-REPRODUCIBLE WHEREAS MODELS HIGHLIGHTED IN **RED** INDICATE THE RESULTS REPRESENT EXTREME OUTLIERS. THE FULL RESULT TABLE WITH STANDARD DEVIATION ACROSS MULTIPLE RUNS CAN BE FOUND AT TABLE XII.

Model		MRR (%)	Hits@1 (%)	Hits@3 (%)	Hits@5 (%)	Hits@10 (%)	MR	AMR (%)
ComplEx	pub	69.2	59.9	75.9		84.		
	R	19.13	10.06	20.82	27.59	38.03	171.16	2.46
ConvE	pub	65.7	55.8	72.3		83.1	51.	
	R	59.56	48.28	66.99	73.27	79.76	50.76	0.73
DistMult	pub	35.				57.7		
	R	26.06	16.45	29.10	35.54	45.00	134.02	1.86
HolE	pub	52.4	40.2	61.3		73.9		
	R	34.15	21.79	39.69	48.06	58.84	193.03	2.71
KG2E	pub					71.5	59.	
	R	0.58	0.11	0.36	0.56	1.01	5779.07	78.40
RotatE	pub	79.7	74.6	83.		88.4	40.	
	R	55.00	41.53	64.14	71.23	78.67	42.28	0.63
SimplE	pub	72.7	66.	77.3		83.8		
	R	0.04	0.01	0.03	0.04	0.06	7395.75	100.02
	O	23.90	11.58	24.16	34.73	54.28	139.34	
	P	0.03	0.01	0.03	0.04	0.06	14652.16	
TransD	pub					77.3	91.	
	R	33.99	21.22	40.48	48.57	58.71	153.37	2.29
TransE	pub					47.1	125.	
	R	26.01	15.23	29.85	37.18	47.34	127.92	1.78
TransH	pub					64.4	87.	
	R	2.54	1.69	2.95	3.29	3.74	6320.02	85.63
	O	2.54	1.69	2.95	3.29	3.74	6320.00	
	P	2.54	1.69	2.95	3.29	3.74	6320.05	
TransR	pub					68.7	77.	
	R	0.65	0.37	0.63	0.78	1.03	6795.95	91.99
	O	0.65	0.37	0.63	0.78	1.03	6795.94	
	P	0.65	0.37	0.63	0.78	1.03	6795.95	
TuckER	pub	79.5	74.1	83.3		89.2		
	R	0.07	0.01	0.02	0.03	0.15	7327.77	99.11

TABLE IX

REPRODUCTION OF STUDIES ON FB15K-237 WITHOUT INDICATING THE STANDARD DEVIATION WHERE **PUB** REFERS TO PUBLISHED RESULTS, **R** TO RESULTS BASED ON THE REALISTIC RANKING, **O** TO RESULTS BASED ON THE OPTIMISTIC RANKING, AND **P** TO RESULTS BASED ON THE PESSIMISTIC RANKING. WE ONLY SHOW THE RESULTS OF THE OPTIMISTIC AND PESSIMISTIC RANKING IN CASE THEY DIFFER FROM THE REALISTIC RANKING. MODELS HIGHLIGHTED IN **BLUE** INDICATE THE EXPERIMENTS ARE SOFT-REPRODUCIBLE WHEREAS MODELS HIGHLIGHTED IN **RED** INDICATE THE RESULTS REPRESENT EXTREME OUTLIERS. THE FULL RESULT TABLE WITH STANDARD DEVIATION ACROSS MULTIPLE RUNS CAN BE FOUND AT TABLE XIII.

Model		MRR (%)	Hits@1 (%)	Hits@3 (%)	Hits@5 (%)	Hits@10 (%)	MR	AMR (%)
ConvE	pub	32.5	23.7	35.6		50.1	244.	
	R	26.93	18.22	29.51	35.98	44.95	255.46	3.73
ConvKB	pub	39.6				51.7	257.	
	R	4.71	3.31	4.04	4.57	7.76	4345.27	61.36
RotatE	pub	33.8	24.1	37.5		53.3	177.	
	R	26.42	17.57	28.97	35.29	44.55	191.92	2.84

TABLE X

REPRODUCTION OF STUDIES ON WN18 WITHOUT INDICATING THE STANDARD DEVIATION WHERE **PUB** REFERS TO PUBLISHED RESULTS, **R** TO RESULTS BASED ON THE REALISTIC RANKING, **O** TO RESULTS BASED ON THE OPTIMISTIC RANKING, AND **P** TO RESULTS BASED ON THE PESSIMISTIC RANKING.

WE ONLY SHOW THE RESULTS OF THE OPTIMISTIC AND PESSIMISTIC RANKING IN CASE THEY DIFFER FROM THE REALISTIC RANKING. MODELS HIGHLIGHTED IN **BLUE** INDICATE THE EXPERIMENTS ARE SOFT-REPRODUCIBLE WHEREAS MODELS HIGHLIGHTED IN **RED** INDICATE THE RESULTS REPRESENT EXTREME OUTLIERS. THE FULL RESULT TABLE WITH STANDARD DEVIATION ACROSS MULTIPLE RUNS CAN BE FOUND AT TABLE XIV.

Model		MRR (%)	Hits@1 (%)	Hits@3 (%)	Hits@5 (%)	Hits@10 (%)	MR	AMR (%)
ComplEx	pub	94.1	93.6	94.5		94.7		
	R	19.49	12.36	20.66	25.24	32.92	452.67	2.21
ConvE	pub	94.3	93.5	94.6		95.6	374.	
	R	88.81	85.14	91.76	93.29	94.85	444.40	2.17
DistMult	pub	83.				94.2		
	R	77.44	67.45	85.94	89.52	92.72	458.64	2.24
HolE	pub	93.8	93.	94.5		94.9		
	R	70.44	59.29	79.29	84.12	88.61	812.64	3.97
	O	70.44	59.29	79.29	84.12	88.61	812.63	
	P	70.44	59.29	79.29	84.12	88.61	812.64	
KG2E	pub					92.8	331.	
	R	3.61	1.35	3.21	4.57	7.02	2708.89	13.25
	O	3.61	1.35	3.21	4.57	7.02	2708.88	
	P	3.61	1.35	3.21	4.57	7.02	2708.89	
RotatE	pub	94.9	94.4	95.2		95.9	309.	
	R	87.29	82.17	91.53	93.44	95.28	123.68	0.61
Simple	pub	94.2	93.9	94.4		94.7		
	R	0.04	0.01	0.03	0.04	0.07	20376.43	99.57
	O	38.48	33.93	39.59	42.76	47.01	384.53	
	P	0.03	0.01	0.03	0.04	0.07	40368.33	
TransD	pub					92.2	212.	
	R	36.22	3.94	65.63	79.64	87.27	444.39	2.17
TransE	pub					89.2	251.	
	R	39.19	9.99	64.74	75.44	84.25	468.24	2.29
TransH	pub					82.3	388.	
	R	0.18	0.04	0.19	0.29	0.39	19678.04	96.16
	O	0.18	0.04	0.19	0.29	0.39	19678.02	
	P	0.18	0.04	0.19	0.29	0.39	19678.06	
TransR	pub					92.	225.	
	R	0.06	0.00	0.04	0.05	0.11	19686.49	96.20
	O	0.06	0.00	0.04	0.05	0.11	19686.49	
	P	0.06	0.00	0.04	0.05	0.11	19686.50	
TuckER	pub	95.3	94.9	95.5		95.8		
	R	0.03	0.00	0.02	0.03	0.04	20622.46	100.78

TABLE XI

REPRODUCTION OF STUDIES ON WN18RR WITHOUT INDICATING THE STANDARD DEVIATION WHERE **PUB** REFERS TO PUBLISHED RESULTS, **R** TO RESULTS BASED ON THE REALISTIC RANKING, **O** TO RESULTS BASED ON THE OPTIMISTIC RANKING, AND **P** TO RESULTS BASED ON THE PESSIMISTIC RANKING. WE ONLY SHOW THE RESULTS OF THE OPTIMISTIC AND PESSIMISTIC RANKING IN CASE THEY DIFFER FROM THE REALISTIC RANKING. MODELS HIGHLIGHTED IN **BLUE** INDICATE THE EXPERIMENTS ARE SOFT-REPRODUCIBLE WHEREAS MODELS HIGHLIGHTED IN **RED** INDICATE THE RESULTS REPRESENT EXTREME OUTLIERS. THE FULL RESULT TABLE WITH STANDARD DEVIATION ACROSS MULTIPLE RUNS CAN BE FOUND AT TABLE XV.

Model		MRR (%)	Hits@1 (%)	Hits@3 (%)	Hits@5 (%)	Hits@10 (%)	MR	AMR (%)
ConvE	pub	43.	4.	44.		52.	4187.	
	R	44.69	40.98	46.49	48.92	51.76	5369.49	26.49
ConvKB	pub	24.8				52.5	2554.	
	R	0.30	0.09	0.21	0.32	0.57	13634.66	67.27
	O	0.30	0.09	0.21	0.32	0.57	13634.65	
	P	0.30	0.09	0.21	0.32	0.57	13634.66	
RotatE	pub	47.6	42.8	49.2		57.1	3340.	
	R	48.40	44.02	50.55	52.98	56.51	4263.32	21.03

TABLE XII

REPRODUCTION OF STUDIES ON FB15K WHERE **PUB** REFERS TO PUBLISHED RESULTS, **R** TO RESULTS BASED ON THE REALISTIC RANKING, **O** TO RESULTS BASED ON THE OPTIMISTIC RANKING, AND **P** TO RESULTS BASED ON THE PESSIMISTIC RANKING. WE ONLY SHOW THE RESULTS OF THE OPTIMISTIC AND PESSIMISTIC RANKING IN CASE THEY DIFFER FROM THE REALISTIC RANKING.

Model		MRR (%)	Hits@1 (%)	Hits@3 (%)	Hits@5 (%)	Hits@10 (%)	MR	AMR (%)
ComplEx	pub	69.2	59.9	75.9		84.		
	R	19.13 \pm 0.45	10.06 \pm 0.42	20.82 \pm 0.67	27.59 \pm 0.94	38.03 \pm 1.02	171.16 \pm 16.05	2.46 \pm 0.28
ConvE	pub	65.7	55.8	72.3		83.1	51.	
	R	59.56 \pm 0.06	48.28 \pm 0.12	66.99 \pm 0.04	73.27 \pm 0.03	79.76 \pm 0.07	50.76 \pm 0.40	0.73 \pm 0.01
DistMult	pub	35.				57.7		
	R	26.06 \pm 0.17	16.45 \pm 0.16	29.10 \pm 0.17	35.54 \pm 0.21	45.00 \pm 0.25	134.02 \pm 1.98	1.86 \pm 0.03
HolE	pub	52.4	40.2	61.3		73.9		
	R	34.15 \pm 0.22	21.79 \pm 0.19	39.69 \pm 0.24	48.06 \pm 0.30	58.84 \pm 0.28	193.03 \pm 7.61	2.71 \pm 0.12
KG2E	pub					71.5	59.	
	R	0.58 \pm 0.07	0.11 \pm 0.04	0.36 \pm 0.08	0.56 \pm 0.10	1.01 \pm 0.14	5779.07 \pm 51.02	78.40 \pm 0.68
RotatE	pub	79.7	74.6	83.		88.4	40.	
	R	55.00 \pm 0.06	41.53 \pm 0.06	64.14 \pm 0.07	71.23 \pm 0.05	78.67 \pm 0.08	42.28 \pm 0.13	0.63 \pm 0.00
Simple	pub	72.7	66.	77.3		83.8		
	R	0.04 \pm 0.00	0.01 \pm 0.00	0.03 \pm 0.00	0.04 \pm 0.00	0.06 \pm 0.01	7395.75 \pm 2.02	100.02 \pm 0.03
	O	23.90 \pm 8.79	11.58 \pm 6.42	24.16 \pm 10.95	34.73 \pm 13.40	54.28 \pm 15.80	139.34 \pm 49.45	
	P	0.03 \pm 0.00	0.01 \pm 0.00	0.03 \pm 0.00	0.04 \pm 0.00	0.06 \pm 0.01	14652.16 \pm 45.71	
TransD	pub					77.3	91.	
	R	33.99 \pm 0.03	21.22 \pm 0.03	40.48 \pm 0.10	48.57 \pm 0.09	58.71 \pm 0.14	153.37 \pm 5.35	2.29 \pm 0.09
TransE	pub					47.1	125.	
	R	26.01 \pm 0.17	15.23 \pm 0.16	29.85 \pm 0.24	37.18 \pm 0.24	47.34 \pm 0.18	127.92 \pm 0.86	1.78 \pm 0.01
TransH	pub					64.4	87.	
	R	2.54 \pm 0.20	1.69 \pm 0.25	2.95 \pm 0.20	3.29 \pm 0.22	3.74 \pm 0.18	6320.02 \pm 30.37	85.63 \pm 0.40
	O	2.54 \pm 0.20	1.69 \pm 0.25	2.95 \pm 0.20	3.29 \pm 0.22	3.74 \pm 0.18	6320.00 \pm 30.37	
	P	2.54 \pm 0.20	1.69 \pm 0.25	2.95 \pm 0.20	3.29 \pm 0.22	3.74 \pm 0.18	6320.05 \pm 30.37	
TransR	pub					68.7	77.	
	R	0.65 \pm 0.02	0.37 \pm 0.00	0.63 \pm 0.04	0.78 \pm 0.06	1.03 \pm 0.07	6795.95 \pm 16.65	91.99 \pm 0.22
	O	0.65 \pm 0.02	0.37 \pm 0.00	0.63 \pm 0.04	0.78 \pm 0.06	1.03 \pm 0.07	6795.94 \pm 16.65	
	P	0.65 \pm 0.02	0.37 \pm 0.00	0.63 \pm 0.04	0.78 \pm 0.06	1.03 \pm 0.07	6795.95 \pm 16.65	
TuckER	pub	79.5	74.1	83.3		89.2		
	R	0.07 \pm 0.02	0.01 \pm 0.00	0.02 \pm 0.00	0.03 \pm 0.01	0.15 \pm 0.17	7327.77 \pm 29.22	99.11 \pm 0.39

TABLE XIII

REPRODUCTION OF STUDIES ON FB15K-237 WHERE **PUB** REFERS TO PUBLISHED RESULTS, **R** TO RESULTS BASED ON THE REALISTIC RANKING, **O** TO RESULTS BASED ON THE OPTIMISTIC RANKING, AND **P** TO RESULTS BASED ON THE PESSIMISTIC RANKING. WE ONLY SHOW THE RESULTS OF THE OPTIMISTIC AND PESSIMISTIC RANKING IN CASE THEY DIFFER FROM THE REALISTIC RANKING.

Model		MRR (%)	Hits@1 (%)	Hits@3 (%)	Hits@5 (%)	Hits@10 (%)	MR	AMR (%)
ConvE	pub	32.5	23.7	35.6		50.1	244.	
	R	26.93 \pm 0.11	18.22 \pm 0.11	29.51 \pm 0.24	35.98 \pm 0.16	44.95 \pm 0.17	255.46 \pm 6.16	3.73 \pm 0.13
ConvKB	pub	39.6				51.7	257.	
	R	4.71 \pm 0.23	3.31 \pm 0.23	4.04 \pm 0.19	4.57 \pm 0.22	7.76 \pm 0.88	4345.27 \pm 46.99	61.36 \pm 0.65
RotatE	pub	33.8	24.1	37.5		53.3	177.	
	R	26.42 \pm 0.04	17.57 \pm 0.06	28.97 \pm 0.05	35.29 \pm 0.09	44.55 \pm 0.06	191.92 \pm 0.31	2.84 \pm 0.00

TABLE XIV

REPRODUCTION OF STUDIES ON WN18 WHERE **PUB** REFERS TO PUBLISHED RESULTS, **R** TO RESULTS BASED ON THE REALISTIC RANKING, **O** TO RESULTS BASED ON THE OPTIMISTIC RANKING, AND **P** TO RESULTS BASED ON THE PESSIMISTIC RANKING. WE ONLY SHOW THE RESULTS OF THE OPTIMISTIC AND PESSIMISTIC RANKING IN CASE THEY DIFFER FROM THE REALISTIC RANKING.

Model		MRR (%)	Hits@1 (%)	Hits@3 (%)	Hits@5 (%)	Hits@10 (%)	MR		AMR (%)
ComplEx	pub	94.1	93.6	94.5		94.7			
	R	19.49 \pm 2.55	12.36 \pm 1.96	20.66 \pm 2.75	25.24 \pm 3.33	32.92 \pm 4.40	452.67 \pm	63.05	2.21 \pm 0.31
ConvE	pub	94.3	93.5	94.6		95.6	374.		
	R	88.81 \pm 0.09	85.14 \pm 0.10	91.76 \pm 0.11	93.29 \pm 0.04	94.85 \pm 0.06	444.40 \pm	14.82	2.17 \pm 0.07
DistMult	pub	83.				94.2			
	R	77.44 \pm 0.22	67.45 \pm 0.34	85.94 \pm 0.21	89.52 \pm 0.25	92.72 \pm 0.18	458.64 \pm	23.96	2.24 \pm 0.12
HolE	pub	93.8	93.	94.5		94.9			
	R	70.44 \pm 0.45	59.29 \pm 0.53	79.29 \pm 0.47	84.12 \pm 0.36	88.61 \pm 0.42	812.64 \pm	28.33	3.97 \pm 0.14
	O	70.44 \pm 0.45	59.29 \pm 0.53	79.29 \pm 0.47	84.12 \pm 0.36	88.61 \pm 0.42	812.63 \pm	28.33	
	P	70.44 \pm 0.45	59.29 \pm 0.53	79.29 \pm 0.47	84.12 \pm 0.36	88.61 \pm 0.42	812.64 \pm	28.34	
KG2E	pub					92.8	331.		
	R	3.61 \pm 0.26	1.35 \pm 0.22	3.21 \pm 0.31	4.57 \pm 0.34	7.02 \pm 0.43	2708.89 \pm	44.57	13.25 \pm 0.22
	O	3.61 \pm 0.26	1.35 \pm 0.22	3.21 \pm 0.31	4.57 \pm 0.34	7.02 \pm 0.43	2708.88 \pm	44.57	
	P	3.61 \pm 0.26	1.35 \pm 0.22	3.21 \pm 0.31	4.57 \pm 0.34	7.02 \pm 0.43	2708.89 \pm	44.57	
RotatE	pub	94.9	94.4	95.2		95.9	309.		
	R	87.29 \pm 0.12	82.17 \pm 0.20	91.53 \pm 0.12	93.44 \pm 0.07	95.28 \pm 0.08	123.68 \pm	1.71	0.61 \pm 0.01
Simple	pub	94.2	93.9	94.4		94.7			
	R	0.04 \pm 0.01	0.01 \pm 0.01	0.03 \pm 0.00	0.04 \pm 0.01	0.07 \pm 0.03	20376.43 \pm	42.30	99.57 \pm 0.21
	O	38.48 \pm 4.00	33.93 \pm 4.32	39.59 \pm 4.67	42.76 \pm 3.73	47.01 \pm 2.66	384.53 \pm	66.45	
	P	0.03 \pm 0.01	0.01 \pm 0.01	0.03 \pm 0.00	0.04 \pm 0.01	0.07 \pm 0.03	40368.33 \pm	114.95	
TransD	pub					92.2	212.		
	R	36.22 \pm 0.12	3.94 \pm 0.27	65.63 \pm 0.55	79.64 \pm 0.43	87.27 \pm 0.41	444.39 \pm	25.61	2.17 \pm 0.13
TransE	pub					89.2	251.		
	R	39.19 \pm 1.21	9.99 \pm 1.82	64.74 \pm 0.91	75.44 \pm 0.48	84.25 \pm 0.33	468.24 \pm	13.64	2.29 \pm 0.07
TransH	pub					82.3	388.		
	R	0.18 \pm 0.04	0.04 \pm 0.02	0.19 \pm 0.10	0.29 \pm 0.14	0.39 \pm 0.11	19678.04 \pm	18.92	96.16 \pm 0.09
	O	0.18 \pm 0.04	0.04 \pm 0.02	0.19 \pm 0.10	0.29 \pm 0.14	0.39 \pm 0.11	19678.02 \pm	18.92	
	P	0.18 \pm 0.04	0.04 \pm 0.02	0.19 \pm 0.10	0.29 \pm 0.14	0.39 \pm 0.11	19678.06 \pm	18.92	
TransR	pub					92.	225.		
	R	0.06 \pm 0.02	0.00 \pm 0.00	0.04 \pm 0.02	0.05 \pm 0.03	0.11 \pm 0.06	19686.49 \pm	100.97	96.20 \pm 0.49
	O	0.06 \pm 0.02	0.00 \pm 0.00	0.04 \pm 0.02	0.05 \pm 0.03	0.11 \pm 0.06	19686.49 \pm	100.97	
	P	0.06 \pm 0.02	0.00 \pm 0.00	0.04 \pm 0.02	0.05 \pm 0.03	0.11 \pm 0.06	19686.50 \pm	100.97	
TuckER	pub	95.3	94.9	95.5		95.8			
	R	0.03 \pm 0.01	0.00 \pm 0.00	0.02 \pm 0.01	0.03 \pm 0.03	0.04 \pm 0.03	20622.46 \pm	153.52	100.78 \pm 0.75

TABLE XV

REPRODUCTION OF STUDIES ON WN18RR WHERE **PUB** REFERS TO PUBLISHED RESULTS, **R** TO RESULTS BASED ON THE REALISTIC RANKING, **O** TO RESULTS BASED ON THE OPTIMISTIC RANKING, AND **P** TO RESULTS BASED ON THE PESSIMISTIC RANKING. WE ONLY SHOW THE RESULTS OF THE OPTIMISTIC AND PESSIMISTIC RANKING IN CASE THEY DIFFER FROM THE REALISTIC RANKING.

Model		MRR (%)	Hits@1 (%)	Hits@3 (%)	Hits@5 (%)	Hits@10 (%)	MR		AMR (%)
ConvE	pub	43.	4.	44.		52.	4187.		
	R	44.69 \pm 0.21	40.98 \pm 0.22	46.49 \pm 0.14	48.92 \pm 0.23	51.76 \pm 0.13	5369.49 \pm	50.92	26.49 \pm 0.25
ConvKB	pub	24.8				52.5	2554.		
	R	0.30 \pm 0.07	0.09 \pm 0.03	0.21 \pm 0.07	0.32 \pm 0.10	0.57 \pm 0.16	13634.66 \pm	714.24	67.27 \pm 3.52
	O	0.30 \pm 0.07	0.09 \pm 0.03	0.21 \pm 0.07	0.32 \pm 0.10	0.57 \pm 0.16	13634.65 \pm	714.24	
	P	0.30 \pm 0.07	0.09 \pm 0.03	0.21 \pm 0.07	0.32 \pm 0.10	0.57 \pm 0.16	13634.66 \pm	714.24	
RotatE	pub	47.6	42.8	49.2		57.1	3340.		
	R	48.40 \pm 0.09	44.02 \pm 0.15	50.55 \pm 0.12	52.98 \pm 0.11	56.51 \pm 0.26	4263.32 \pm	90.33	21.03 \pm 0.45

TABLE XVI
MODEL SIZES IN BYTES FOR THE BEST REPORTED CONFIGURATIONS STUDIED FOR THE THE REPRODUCIBILITY STUDY.

Dataset Model	FB15K	FB15K-237	WN18	WN18RR
ComplEx	26.1 MB	-	49.2 MB	-
ConvE	22.5 MB	20.3 MB	41.2 MB	40.9 MB
ConvKB	-	5.9 MB	-	8.2 MB
DistMult	6.5 MB	-	16.4 MB	-
HolE	9.8 MB	-	24.6 MB	-
KG2E	6.5 MB	-	16.4 MB	-
RotatE	130.4 MB	117.9 MB	163.8 MB	162.3 MB
Simple	26.1 MB	-	65.5 MB	-
TransD	6.5 MB	-	16.4 MB	-
TransE	3.3 MB	-	3.3 MB	-
TransH	7.1 MB	-	8.2 MB	-
TransR	16.7 MB	-	8.4 MB	-
TuckER	46.1 MB	-	37.6 MB	-

ADDITIONAL RESULTS FROM BENCHMARKING STUDY

TABLE XVII
PARETO-OPTIMAL MODELS FOR FB15K-237 REGARDING MODEL BYTES AND HITS@10

Model	Loss	Training Approach	Inverse Relations	Model Bytes	Hits@10 (%)
RotatE	NSSAL	sLCWA	False	28.8 MiB	48.177
RotatE	NSSAL	sLCWA	True	14.6 MiB	47.710
DistMult	CEL	LCWA	True	3.7 MiB	45.968
TransE	SPL	LCWA	False	3.6 MiB	43.928
UM	MRL	sLCWA	False	3.5 MiB	3.217
UM	MRL	sLCWA	True	3.5 MiB	2.958

TABLE XVIII
PARETO-OPTIMAL MODELS FOR KINSHIPS REGARDING MODEL BYTES AND HITS@10

Model	Loss	Training Approach	Inverse Relations	Model Bytes	Hits@10 (%)
TuckER	SPL	LCWA	True	32.1 MiB	98.696
RotatE	MRL	sLCWA	False	258.0 KiB	98.464
SimplE	BCEL	LCWA	True	77.0 KiB	98.371
ProjE	BCEL	sLCWA	True	39.3 KiB	96.089
ProjE	SPL	sLCWA	False	33.0 KiB	95.251
HolE	SPL	LCWA	False	32.2 KiB	87.989
UM	SPL	LCWA	False	26.0 KiB	11.872
UM	SPL	sLCWA	True	26.0 KiB	5.447

TABLE XIX
PARETO-OPTIMAL MODELS FOR WN18RR REGARDING MODEL BYTES AND HITS@10

Model	Loss	Training Approach	Inverse Relations	Model Bytes	Hits@10 (%)
RotatE	SPL	LCWA	True	79.3 MiB	60.174
RotatE	BCEL	LCWA	True	19.8 MiB	59.285
ConvE	SPL	LCWA	True	10.6 MiB	53.061
ConvKB	BCEL	sLCWA	False	5.0 MiB	41.860
ConvKB	NSSAL	sLCWA	False	2.5 MiB	20.092

TABLE XX
PARETO-OPTIMAL MODELS FOR YAGO3-10 REGARDING MODEL BYTES AND HITS@10

Model	Loss	Training Approach	Inverse Relations	Model Bytes	Hits@10 (%)
RotatE	NSSAL	sLCWA	True	240.7 MiB	62.786
ComplEx	SPL	sLCWA	True	120.3 MiB	61.000
ERMLP	SPL	sLCWA	True	60.4 MiB	58.752
ConvKB	SPL	sLCWA	False	30.1 MiB	52.710
ConvKB	NSSAL	sLCWA	False	30.1 MiB	51.445
DistMult	SPL	sLCWA	True	30.1 MiB	49.950
TransE	BCEL	sLCWA	False	30.1 MiB	14.251

TABLE XXI
BEST CONFIGURATION FOR EACH MODEL IN FB15K-237

Model	Loss	Training Approach	Inverse Relations	Hits@10 (%)
ComplEx	CEL	LCWA	True	0.430571
DistMult	CEL	LCWA	True	0.459683
ERMLP	BCEL	LCWA	True	0.421494
HolE	CEL	LCWA	True	0.410021
KG2E	SPL	LCWA	True	0.435463
NTN	SPL	sLCWA	False	0.194784
ProjE	CEL	LCWA	True	0.404223
RESCAL	CEL	LCWA	True	0.447206
RotatE	NSSAL	sLCWA	False	0.481774
Simple	BCEL	LCWA	True	0.395807
TransD	MRL	sLCWA	True	0.397397
TransE	CEL	LCWA	True	0.444001
TransH	MRL	sLCWA	False	0.337215
TransR	CEL	LCWA	True	0.383183
TuckER	SPL	LCWA	True	0.452833
UM	CEL	LCWA	False	0.080414

TABLE XXII
BEST CONFIGURATION FOR EACH MODEL IN KINSHIPS

Model	Loss	Training Approach	Inverse Relations	Hits@10 (%)
ComplEx	NSSAL	sLCWA	True	0.982775
ConvE	BCEL	LCWA	True	0.982775
ConvKB	NSSAL	sLCWA	True	0.964153
DistMult	CEL	LCWA	True	0.924581
ERMLP	NSSAL	sLCWA	True	0.973929
HolE	CEL	LCWA	True	0.933892
KG2E	MRL	sLCWA	True	0.912942
NTN	BCEL	sLCWA	True	0.938547
ProjE	SPL	sLCWA	True	0.960894
RESCAL	SPL	sLCWA	False	0.976257
RotatE	MRL	sLCWA	False	0.984637
SE	NSSAL	sLCWA	True	0.978585
Simple	BCEL	LCWA	True	0.983706
TransD	CEL	LCWA	True	0.467877
TransE	CEL	LCWA	True	0.920391
TransH	CEL	LCWA	True	0.520019
TransR	CEL	LCWA	True	0.713687
TuckER	SPL	LCWA	True	0.986965
UM	SPL	LCWA	False	0.118715

TABLE XXIII
BEST CONFIGURATION FOR EACH MODEL IN WN18RR

Model	Loss	Training Approach	Inverse Relations	Hits@10 (%)
ComplEx	CEL	LCWA	False	0.531464
ConvE	CEL	LCWA	True	0.563440
ConvKB	NSSAL	sLCWA	True	0.445964
DistMult	CEL	LCWA	True	0.527018
ERMLP	BCEL	sLCWA	True	0.478454
HolE	CEL	LCWA	False	0.501026
KG2E	SPL	LCWA	False	0.513509
NTN	MRL	sLCWA	False	0.310021
ProjE	CEL	LCWA	True	0.514535
RESCAL	CEL	LCWA	False	0.536423
RotatE	SPL	LCWA	True	0.601744
SE	SPL	sLCWA	False	0.430404
Simple	CEL	LCWA	True	0.507866
TransD	BCEL	sLCWA	True	0.454343
TransE	SPL	LCWA	False	0.570280
TransH	MRL	sLCWA	False	0.479309
TransR	MRL	sLCWA	False	0.423906
TuckER	CEL	LCWA	True	0.548393
UM	SPL	LCWA	True	0.450410

TABLE XXIV
BEST CONFIGURATION FOR EACH MODEL IN YAGO3-10

Model	Loss	Training Approach	Inverse Relations	Hits@10 (%)
ComplEx	BCEL	sLCWA	True	0.621738
ConvKB	SPL	sLCWA	True	0.562224
DistMult	BCEL	sLCWA	False	0.553493
ERMLP	SPL	sLCWA	True	0.587515
HolE	BCEL	sLCWA	False	0.584906
RESCAL	SPL	sLCWA	True	0.544661
RotatE	NSSAL	sLCWA	True	0.627860
SE	NSSAL	sLCWA	True	0.291650
TransD	MRL	sLCWA	False	0.348756
TransE	MRL	sLCWA	True	0.477017

training_approach = LCWA				training_approach = sLCWA				inverse_relations = False	
	BCEL	CEL	SPL		BCEL	MRL	NSSAL		SPL
ComplEx	29.19%	97.18%	18.95%	ComplEx	97.53%	96.86%	97.56%		97.79%
ConvE	93.83%	94.65%	93.76%	ConvE	92.78%	95.72%	96.23%		94.97%
ConvKB	20.74%	70.76%	19.65%	ConvKB	78.56%	92.11%	88.41%		89.62%
DistMult	10.20%	81.15%	10.59%	DistMult	57.96%	85.10%	57.31%		56.15%
ERMLP	72.56%	57.45%	65.50%	ERMLP	88.20%	88.97%	89.99%		90.55%
HolE	86.10%	88.08%	85.50%	HolE	86.29%	86.15%	85.50%		85.71%
KG2E	10.10%	67.06%	25.44%	KG2E	11.06%	90.57%	88.90%		51.44%
NTN	10.71%	10.03%	9.92%	NTN	9.57%	10.66%	10.15%		10.43%
ProjE	17.30%	82.80%	16.34%	ProjE	77.03%	88.64%	91.57%		86.78%
RESICAL	30.98%	91.18%	89.20%	RESICAL		84.68%	92.06%		
RotatE	10.38%	96.58%	9.87%	RotatE	87.50%	97.30%	95.23%		86.55%
SE	95.04%	94.27%	95.00%	SE			97.04%		
Simple	48.11%	93.53%	45.81%	Simple	93.48%	91.43%	93.97%		94.18%
TransD	24.23%	36.73%	21.30%	TransD	35.61%	35.59%	28.89%		30.03%
TransE	70.37%	83.64%	61.15%	TransE	68.11%	86.24%	88.87%		68.32%
TransR	55.31%	61.50%	52.86%	TransR	70.04%	70.46%	63.36%		69.06%
TuckER	94.79%	96.32%	94.46%	TuckER	96.44%	97.70%			
UM	8.80%	7.75%	9.31%	UM	9.92%	5.40%	6.24%		8.19%
	BCEL	CEL	SPL		BCEL	MRL	NSSAL	SPL	
ComplEx	82.82%	97.86%	89.13%	ComplEx	97.46%	96.51%	97.72%	97.16%	
ConvE	97.77%	98.00%	97.39%	ConvE	94.37%	86.99%	96.83%	97.23%	
ConvKB	22.74%	89.04%	21.28%	ConvKB	90.95%	94.93%	88.87%	84.29%	
DistMult	10.31%	87.62%	10.82%	DistMult	65.11%	86.01%	57.17%	55.84%	
ERMLP	88.92%	89.66%	87.52%	ERMLP	94.23%	94.18%	94.39%	93.58%	
HolE	86.80%	92.55%	86.71%	HolE	85.73%	86.36%	86.03%	85.96%	
KG2E	10.92%	87.10%	30.75%	KG2E	10.15%	91.11%	89.71%	80.98%	
NTN	9.94%	10.29%	10.34%	NTN	10.15%	10.06%	9.89%	9.15%	
ProjE	25.63%	92.04%	23.81%	ProjE	89.27%	90.55%	94.11%	91.39%	
RESICAL	93.48%	94.83%	94.46%	RESICAL		93.13%	96.49%		
RotatE	9.85%	96.86%	10.34%	RotatE	86.94%	96.93%	95.88%	86.62%	
SE	95.90%	97.23%	96.11%	SE	96.86%		97.74%	96.69%	
Simple	80.07%	96.00%	79.59%	Simple	94.44%	92.41%	95.18%	94.86%	
TransD	23.79%	44.55%	30.26%	TransD	37.50%	40.46%	28.93%	27.56%	
TransE	72.95%	91.13%	65.13%	TransE	67.76%	85.80%	87.92%	69.32%	
TransR	55.00%	68.67%	55.05%	TransR	57.54%	69.16%	67.16%	64.94%	
TuckER	97.51%	98.04%	97.35%	TuckER	97.97%	98.37%	92.43%	97.77%	
UM	9.52%	7.01%	9.78%	UM	9.36%	5.96%	4.77%	6.08%	
	BCEL	CEL	SPL		BCEL	MRL	NSSAL	SPL	

training_approach = LCWA				training_approach = sLCWA				inverse_relations = True	
	BCEL	CEL	SPL		BCEL	MRL	NSSAL		SPL
ComplEx	82.82%	97.86%	89.13%	ComplEx	97.46%	96.51%	97.72%		97.16%
ConvE	97.77%	98.00%	97.39%	ConvE	94.37%	86.99%	96.83%		97.23%
ConvKB	22.74%	89.04%	21.28%	ConvKB	90.95%	94.93%	88.87%		84.29%
DistMult	10.31%	87.62%	10.82%	DistMult	65.11%	86.01%	57.17%		55.84%
ERMLP	88.92%	89.66%	87.52%	ERMLP	94.23%	94.18%	94.39%		93.58%
HolE	86.80%	92.55%	86.71%	HolE	85.73%	86.36%	86.03%		85.96%
KG2E	10.92%	87.10%	30.75%	KG2E	10.15%	91.11%	89.71%		80.98%
NTN	9.94%	10.29%	10.34%	NTN	10.15%	10.06%	9.89%		9.15%
ProjE	25.63%	92.04%	23.81%	ProjE	89.27%	90.55%	94.11%		91.39%
RESICAL	93.48%	94.83%	94.46%	RESICAL		93.13%	96.49%		
RotatE	9.85%	96.86%	10.34%	RotatE	86.94%	96.93%	95.88%		86.62%
SE	95.90%	97.23%	96.11%	SE	96.86%		97.74%		96.69%
Simple	80.07%	96.00%	79.59%	Simple	94.44%	92.41%	95.18%		94.86%
TransD	23.79%	44.55%	30.26%	TransD	37.50%	40.46%	28.93%		27.56%
TransE	72.95%	91.13%	65.13%	TransE	67.76%	85.80%	87.92%		69.32%
TransR	55.00%	68.67%	55.05%	TransR	57.54%	69.16%	67.16%		64.94%
TuckER	97.51%	98.04%	97.35%	TuckER	97.97%	98.37%	92.43%		97.77%
UM	9.52%	7.01%	9.78%	UM	9.36%	5.96%	4.77%		6.08%
	BCEL	CEL	SPL		BCEL	MRL	NSSAL	SPL	

Fig. 27. Results for all configurations on Kinships based on Adadelta. **BCEL** refers to the binary cross entropy loss, **CEL** to the cross entropy loss, **MRL** to the margin ranking loss, **NSSAL** refers to the negative sampling self-adversarial loss, **SPL** to the softplus loss, **LCWA** to the local closed world assumption training approach and **sLCWA** to the stochastic local closed world assumption training approach.

training_approach = LCWA				training_approach = sLCWA				inverse_relations = False
	BCEL	CEL	SPL		BCEL	MRL	NSSAL	SPL
ComplEx	93.27%	96.86%	92.74%	ComplEx	97.56%	95.74%	96.86%	97.28%
ConvE	95.69%	94.69%	94.95%	ConvE	96.72%	95.46%	68.76%	96.55%
ConvKB	94.09%	88.01%	92.46%	ConvKB	79.70%	94.93%	94.51%	94.37%
DistMult	85.24%	88.45%	84.66%	DistMult	85.68%	85.71%	85.73%	86.01%
ERMLP	90.25%	69.93%	88.71%	ERMLP	91.97%	93.13%	94.48%	94.67%
HolE	86.82%	85.78%	87.55%	HolE	85.80%	85.68%	85.61%	85.61%
KG2E	10.57%	16.55%	14.13%	KG2E	10.75%	88.20%	16.81%	13.52%
NTN	83.52%	86.87%	84.26%	NTN	82.47%	85.20%	61.71%	89.39%
ProjE	91.78%	92.48%	86.52%	ProjE	93.95%	91.22%	92.25%	94.74%
RESICAL	54.52%	94.97%	83.05%	RESICAL	93.53%	90.57%	95.27%	97.32%
RotatE	97.67%	97.81%	89.39%	RotatE	93.76%	98.46%	98.32%	93.34%
SE	93.65%	94.09%	93.72%	SE	96.44%	96.18%	95.58%	96.23%
Simple	96.25%	97.00%	91.41%	Simple	97.84%	95.55%	97.39%	97.77%
TransD	30.63%	38.64%	26.49%	TransD	36.76%	41.99%	33.26%	35.06%
TransE	63.94%	79.07%	65.32%	TransE	68.04%	78.49%	87.80%	67.43%
TransH	26.93%	45.74%	26.89%	TransH	46.32%	47.46%	47.21%	38.62%
TransR	62.57%	64.83%	62.20%	TransR	68.67%	71.04%	66.81%	70.83%
Tucker	97.21%	97.53%	96.88%	Tucker	97.81%	97.58%		97.07%
UM	10.17%	9.40%	11.45%	UM	9.43%	7.05%	7.96%	8.36%
								inverse_relations = True
	BCEL	CEL	SPL		BCEL	MRL	NSSAL	SPL
ComplEx	96.51%	97.84%	94.81%	ComplEx	97.77%	94.95%	97.37%	97.67%
ConvE	98.11%	97.74%	98.00%	ConvE	23.37%	69.95%	44.79%	94.74%
ConvKB	95.37%	94.90%	94.69%	ConvKB	95.02%	96.00%	95.90%	96.18%
DistMult	85.34%	92.18%	84.36%	DistMult	85.94%	85.08%	84.50%	86.22%
ERMLP	94.69%	94.69%	95.00%	ERMLP	96.83%	95.41%	96.88%	96.86%
HolE	87.57%	92.36%	87.29%	HolE	86.17%	85.85%	86.43%	85.99%
KG2E	10.68%	19.44%	14.46%	KG2E	11.17%	89.43%	69.58%	52.23%
NTN	88.31%	90.78%	88.41%	NTN	93.51%	87.80%	76.89%	11.73%
ProjE	94.81%	94.11%	91.04%	ProjE	95.62%	93.20%	95.16%	95.25%
RESICAL	83.99%	96.65%	88.78%	RESICAL	88.36%	90.27%	95.32%	97.42%
RotatE	95.25%	97.95%	91.53%	RotatE	93.62%	98.28%	98.09%	93.76%
SE	96.11%	96.39%	95.76%	SE	96.25%	95.95%	95.65%	96.42%
Simple	97.72%	98.04%	93.44%	Simple	98.00%	94.44%	97.67%	97.95%
TransD	38.83%	46.51%	38.99%	TransD	33.92%	41.76%	33.54%	31.10%
TransE	67.71%	86.36%	63.59%	TransE	66.34%	85.17%	80.82%	66.39%
TransH	35.50%	51.16%	35.50%	TransH	34.33%	47.18%	32.59%	32.59%
TransR	69.48%	71.35%	69.83%	TransR	68.99%	69.74%	68.30%	69.48%
Tucker	98.51%	98.56%	98.70%	Tucker	98.18%	94.30%	97.79%	98.32%
UM	9.10%	10.61%	11.08%	UM	9.68%	6.54%	9.24%	8.71%
								inverse_relations = True
	BCEL	CEL	SPL		BCEL	MRL	NSSAL	SPL

Fig. 28. Results for all configurations on Kinships based on Adam. **BCEL** refers to the binary cross entropy loss, **CEL** to the cross entropy loss, **MRL** to the margin ranking loss, **NSSAL** refers to the negative sampling self-adversarial loss, **SPL** to the softplus loss, **LCWA** to the local closed world assumption training approach and **sLCWA** to the stochastic local closed world assumption training approach.

training approach = LCWA				training approach = sLCWA				inverse_relations = False	
	BCEL	CEL	SPL		BCEL	MRL	NSSAL		SPL
ComplEx	45.64%	53.15%	41.04%	ComplEx	43.37%	42.36%	41.76%		43.02%
ConvE	51.52%	48.72%	48.99%	ConvE	1.30%	1.44%	3.06%		9.40%
ConvKB				ConvKB	41.86%	39.91%	20.09%		19.27%
DistMult	43.04%	48.61%	45.52%	DistMult	48.77%	47.49%	49.33%		44.07%
ERMLP	23.34%	32.05%	21.24%	ERMLP	27.33%	25.43%	16.60%		27.26%
HolE	46.99%	50.10%	38.97%	HolE	45.76%	41.23%	43.84%		46.00%
KG2E	0.02%	42.80%	51.35%	KG2E	34.18%	44.99%	46.34%		46.46%
NTN		1.25%		NTN	0.82%	31.00%			0.74%
ProJE	45.25%	48.38%	37.48%	ProJE	42.01%	40.54%	41.36%		41.71%
RESCAL	41.06%	53.64%	38.92%	RESCAL	38.78%	36.20%	42.78%		40.49%
RotatE	58.72%	52.77%	58.12%	RotatE	50.43%	50.77%	57.80%		50.74%
SE				SE	41.67%				43.04%
Simple	45.57%	49.38%	38.01%	Simple	42.68%	38.56%	40.17%		42.31%
TransD	0.10%	15.80%	0.10%	TransD	44.53%	39.45%	36.70%		44.77%
TransE	3.83%	34.06%	57.03%	TransE	43.40%	48.41%	49.81%		42.51%
TransH	1.95%	14.95%	0.77%	TransH	24.45%	47.93%	3.49%		36.32%
TransR	1.30%	15.17%	0.46%	TransR	34.99%	42.39%	33.24%		35.19%
TuckER	50.12%	51.06%	49.35%	TuckER		46.12%			45.54%
UM	44.13%	40.94%	45.01%	UM	40.27%	39.38%	41.31%	39.93%	
	BCEL	CEL	SPL		BCEL	MRL	NSSAL	SPL	
ComplEx	43.52%	11.54%	36.68%	ComplEx	40.82%	41.40%	41.47%	41.91%	
ConvE	53.35%	56.34%	53.06%	ConvE	13.08%	0.07%	40.22%	35.43%	
ConvKB				ConvKB	40.83%	41.26%	44.60%	41.55%	
DistMult	46.08%	52.70%	43.83%	DistMult	49.26%	45.54%	48.55%	45.09%	
ERMLP	42.79%	46.34%	41.32%	ERMLP	47.85%	41.98%	46.56%	47.57%	
HolE	44.39%	30.73%	33.45%	HolE	46.87%	39.30%	42.97%	45.23%	
KG2E	0.05%	48.19%	50.48%	KG2E	0.03%	42.68%	43.79%	45.76%	
NTN		0.00%		NTN	22.64%	25.39%		0.02%	
ProJE	44.13%	51.45%	42.49%	ProJE	42.78%	42.27%	43.40%	41.55%	
RESCAL	35.65%	52.87%	40.49%	RESCAL	39.65%	37.67%	41.59%	42.29%	
RotatE	59.29%	54.60%	60.17%	RotatE	48.65%	47.47%	57.97%	49.09%	
SE		2.56%		SE	40.46%			41.31%	
Simple	45.23%	50.79%	40.00%	Simple	41.93%	38.39%	38.49%	42.48%	
TransD	0.10%	29.21%	0.03%	TransD	45.43%	44.72%	30.49%	41.40%	
TransE	56.19%	46.31%	23.22%	TransE	44.36%	48.96%	50.60%	42.08%	
TransH	1.90%	13.85%	1.54%	TransH	33.98%	35.64%	3.86%	3.97%	
TransR	0.12%	37.96%	0.14%	TransR	32.44%	7.88%	27.62%	34.15%	
TuckER	52.75%	54.84%	51.25%	TuckER		50.55%		43.86%	
UM	43.74%	42.66%	45.04%	UM	39.57%	40.10%	41.45%	39.69%	
	BCEL	CEL	SPL		BCEL	MRL	NSSAL	SPL	

training approach = LCWA				training approach = sLCWA				inverse_relations = True	
	BCEL	CEL	SPL		BCEL	MRL	NSSAL		SPL
ComplEx	43.52%	11.54%	36.68%	ComplEx	40.82%	41.40%	41.47%		41.91%
ConvE	53.35%	56.34%	53.06%	ConvE	13.08%	0.07%	40.22%		35.43%
ConvKB				ConvKB	40.83%	41.26%	44.60%		41.55%
DistMult	46.08%	52.70%	43.83%	DistMult	49.26%	45.54%	48.55%		45.09%
ERMLP	42.79%	46.34%	41.32%	ERMLP	47.85%	41.98%	46.56%		47.57%
HolE	44.39%	30.73%	33.45%	HolE	46.87%	39.30%	42.97%		45.23%
KG2E	0.05%	48.19%	50.48%	KG2E	0.03%	42.68%	43.79%		45.76%
NTN		0.00%		NTN	22.64%	25.39%			0.02%
ProJE	44.13%	51.45%	42.49%	ProJE	42.78%	42.27%	43.40%		41.55%
RESCAL	35.65%	52.87%	40.49%	RESCAL	39.65%	37.67%	41.59%		42.29%
RotatE	59.29%	54.60%	60.17%	RotatE	48.65%	47.47%	57.97%		49.09%
SE		2.56%		SE	40.46%				41.31%
Simple	45.23%	50.79%	40.00%	Simple	41.93%	38.39%	38.49%		42.48%
TransD	0.10%	29.21%	0.03%	TransD	45.43%	44.72%	30.49%		41.40%
TransE	56.19%	46.31%	23.22%	TransE	44.36%	48.96%	50.60%		42.08%
TransH	1.90%	13.85%	1.54%	TransH	33.98%	35.64%	3.86%		3.97%
TransR	0.12%	37.96%	0.14%	TransR	32.44%	7.88%	27.62%		34.15%
TuckER	52.75%	54.84%	51.25%	TuckER		50.55%			43.86%
UM	43.74%	42.66%	45.04%	UM	39.57%	40.10%	41.45%	39.69%	
	BCEL	CEL	SPL		BCEL	MRL	NSSAL	SPL	

Fig. 29. Results for all configurations on WN18RR based on Adam. **BCEL** refers to the binary cross entropy loss, **CEL** to the cross entropy loss, **MRL** to the margin ranking loss, **NSSAL** refers to the negative sampling self-adversarial loss, **SPL** to the softplus loss, **LCWA** to the local closed world assumption training approach and **sLCWA** to the stochastic local closed world assumption training approach.

training approach = LCWA				training approach = sLCWA				inverse_relations = False
	BCEL	CEL	SPL		BCEL	MRL	NSSAL	SPL
ComplEx	26.95%	38.79%	21.61%	ComplEx	34.19%	29.64%	28.54%	31.96%
DistMult	33.31%	39.07%	32.29%	DistMult	31.90%	37.56%	33.55%	33.52%
ERMLP	25.96%	27.31%	25.07%	ERMLP	35.54%	35.48%	28.95%	32.82%
HolE	37.66%	31.91%	32.15%	HolE	34.49%	28.81%	30.37%	33.48%
KG2E	0.06%	21.82%	40.25%	KG2E	2.95%	36.54%	36.33%	40.46%
NTN		18.74%		NTN	2.22%	9.56%	0.05%	19.48%
ProJE	30.42%	28.39%	23.10%	ProJE	28.45%	31.35%	26.04%	28.14%
RESICAL	26.37%	35.99%	20.27%	RESICAL	25.28%	32.14%	30.56%	33.59%
Rotate	45.66%	41.66%	43.66%	Rotate	35.80%	39.61%	48.18%	36.51%
Simple	22.08%	30.66%	20.12%	Simple	26.89%	21.03%	29.66%	22.10%
TransD	4.03%	26.01%	1.03%	TransD	27.75%	32.95%	24.80%	28.65%
TransE	43.12%	33.19%	43.77%	TransE	29.43%	43.92%	40.28%	33.82%
TransH	15.38%	21.35%	21.37%	TransH	26.39%	33.72%	25.38%	25.42%
TransR	10.26%	21.16%	9.59%	TransR		33.93%	7.35%	
TuckER	33.53%	40.71%	37.55%	TuckER				
UM	6.48%	8.04%	7.11%	UM	5.85%	3.22%	5.58%	5.88%
								inverse_relations = True
	BCEL	CEL	SPL		BCEL	MRL	NSSAL	SPL
ComplEx	33.35%	43.06%	26.77%	ComplEx	30.59%	32.38%	27.54%	25.80%
DistMult	38.83%	45.97%	37.32%	DistMult	32.15%	35.65%	33.24%	32.54%
ERMLP	42.15%	39.51%	37.93%	ERMLP	33.55%	35.28%	30.34%	35.39%
HolE	38.34%	41.00%	32.67%	HolE	34.37%	29.62%	30.90%	34.69%
KG2E	0.05%	36.28%	43.55%	KG2E	0.21%	34.89%	32.45%	38.36%
NTN	18.29%	0.97%		NTN	9.81%	2.97%	0.84%	4.56%
ProJE	40.18%	40.42%	32.10%	ProJE	24.80%	33.77%	22.67%	23.16%
RESICAL	43.81%	44.72%	29.63%	RESICAL	29.14%	31.21%	25.65%	31.40%
Rotate	42.29%	45.62%	44.30%	Rotate	35.36%	28.68%	47.71%	35.86%
Simple	39.58%	36.74%	31.29%	Simple	27.97%	30.32%	27.68%	29.02%
TransD	2.94%	28.35%	2.97%	TransD	24.31%	39.74%	24.34%	28.17%
TransE	38.07%	44.40%	41.22%	TransE	28.60%	41.37%	38.39%	33.30%
TransH	25.76%	24.61%	26.75%	TransH	23.82%	27.17%	22.14%	24.28%
TransR	14.81%	38.32%	11.64%	TransR		32.25%	11.21%	
TuckER	39.11%	43.90%	45.28%	TuckER				
UM	6.49%	7.72%	7.07%	UM	5.94%	2.96%	5.74%	5.93%

Fig. 30. Results for all configurations on FB15K-237 based on Adam. **BCEL** refers to the binary cross entropy loss, **CEL** to the cross entropy loss, **MRL** to the margin ranking loss, **NSSAL** refers to the negative sampling self-adversarial loss, **SPL** to the softplus loss, **LCWA** to the local closed world assumption training approach and **sLCWA** to the stochastic local closed world assumption training approach.

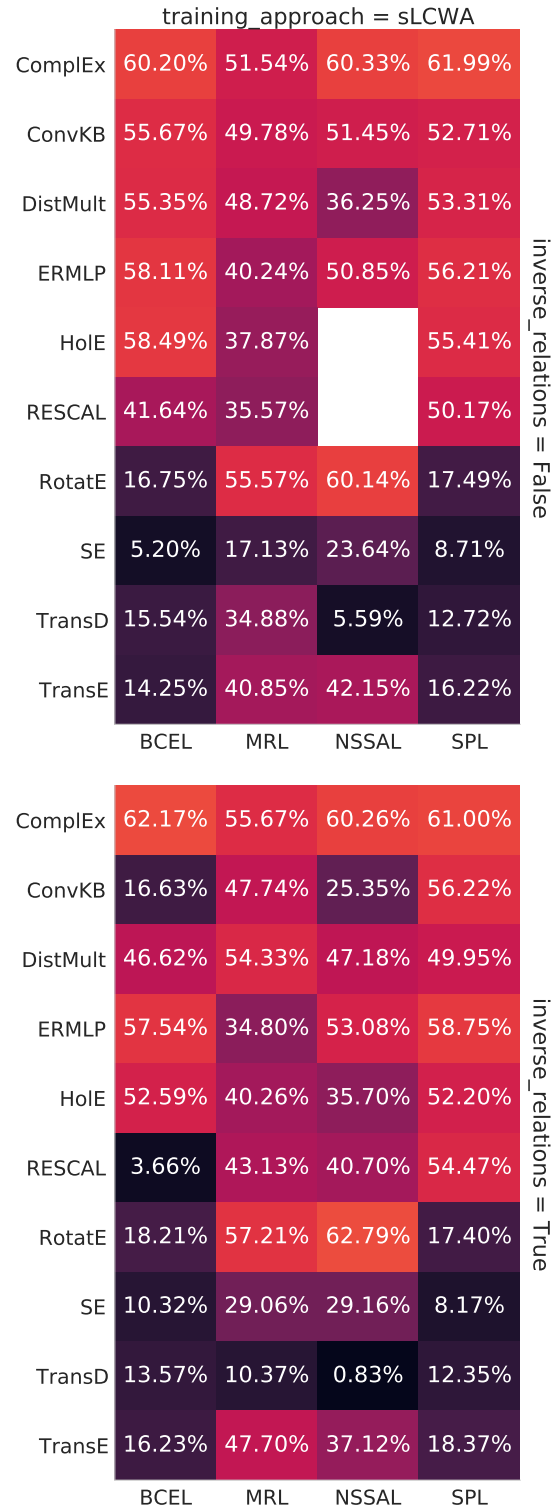


Fig. 31. Results for all configurations on YAGO3-10 based on Adam. **BCEL** refers to the binary cross entropy loss, **CEL** to the cross entropy loss, **MRL** to the margin ranking loss, **NSSAL** refers to the negative sampling self-adversarial loss, **SPL** to the softplus loss, **LCWA** to the local closed world assumption training approach and **sLCWA** to the stochastic local closed world assumption training approach.

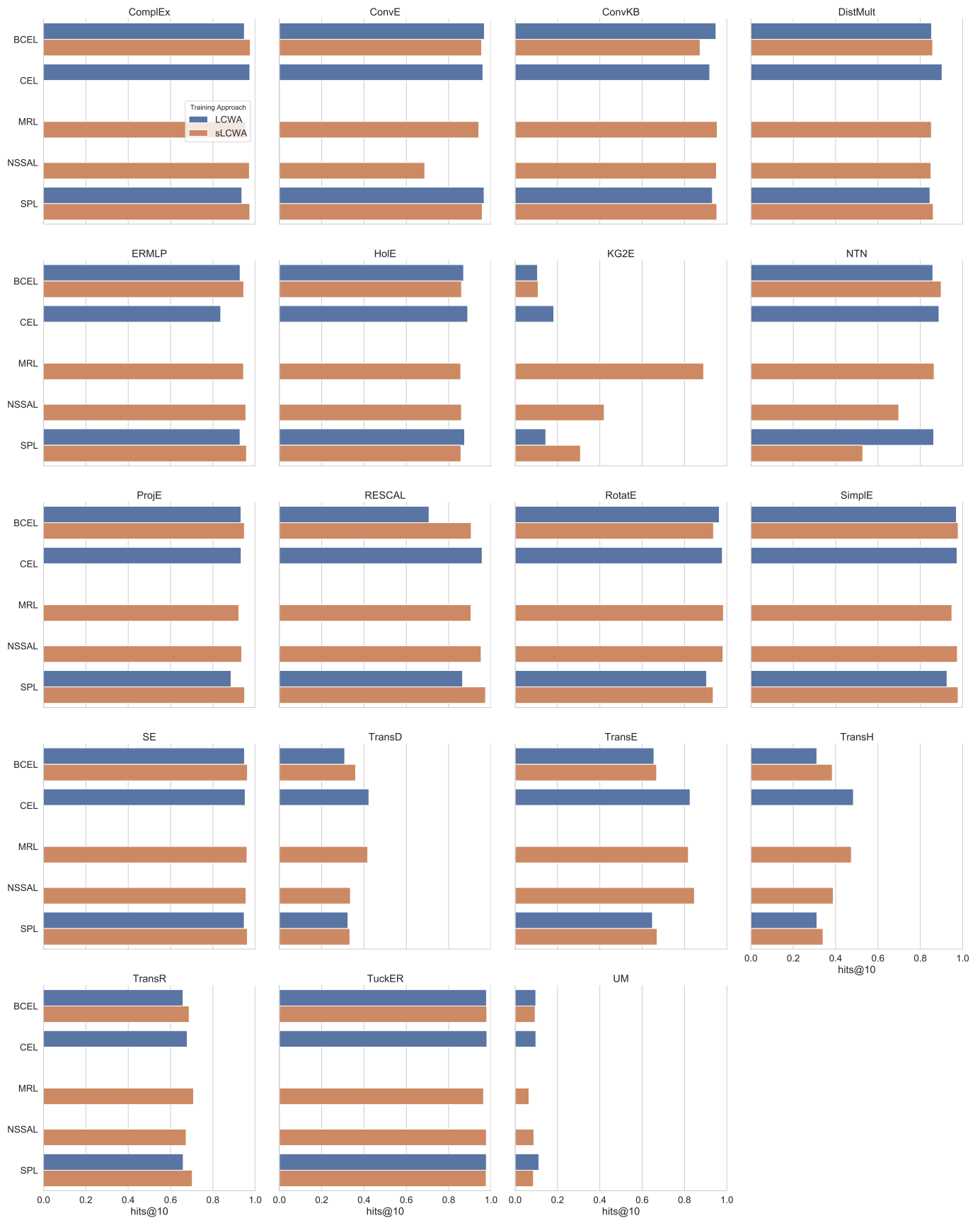


Fig. 32. Impact of the training approach on the performance for a fixed interaction model and loss function for the Kinships dataset (results are aggregated based on the medians). **BCEL** refers to the binary cross entropy loss, **CEL** to the cross entropy loss, **MRL** to the margin ranking loss, **NSSAL** refers to the negative sampling self-adversarial loss, **SPL** to the softplus loss, **LCWA** to the local closed world assumption training approach and **sLCWA** to the stochastic local closed world assumption training approach.



Fig. 33. Impact of the training approach on the performance for a fixed interaction model and loss function for the WN18RR dataset (results are aggregated based on the medians). **BCEL** refers to the binary cross entropy loss, **CEL** to the cross entropy loss, **MRL** to the margin ranking loss, **NSSAL** refers to the negative sampling self-adversarial loss, **SPL** to the softplus loss, **LCWA** to the local closed world assumption training approach and **sLCWA** to the stochastic local closed world assumption training approach.

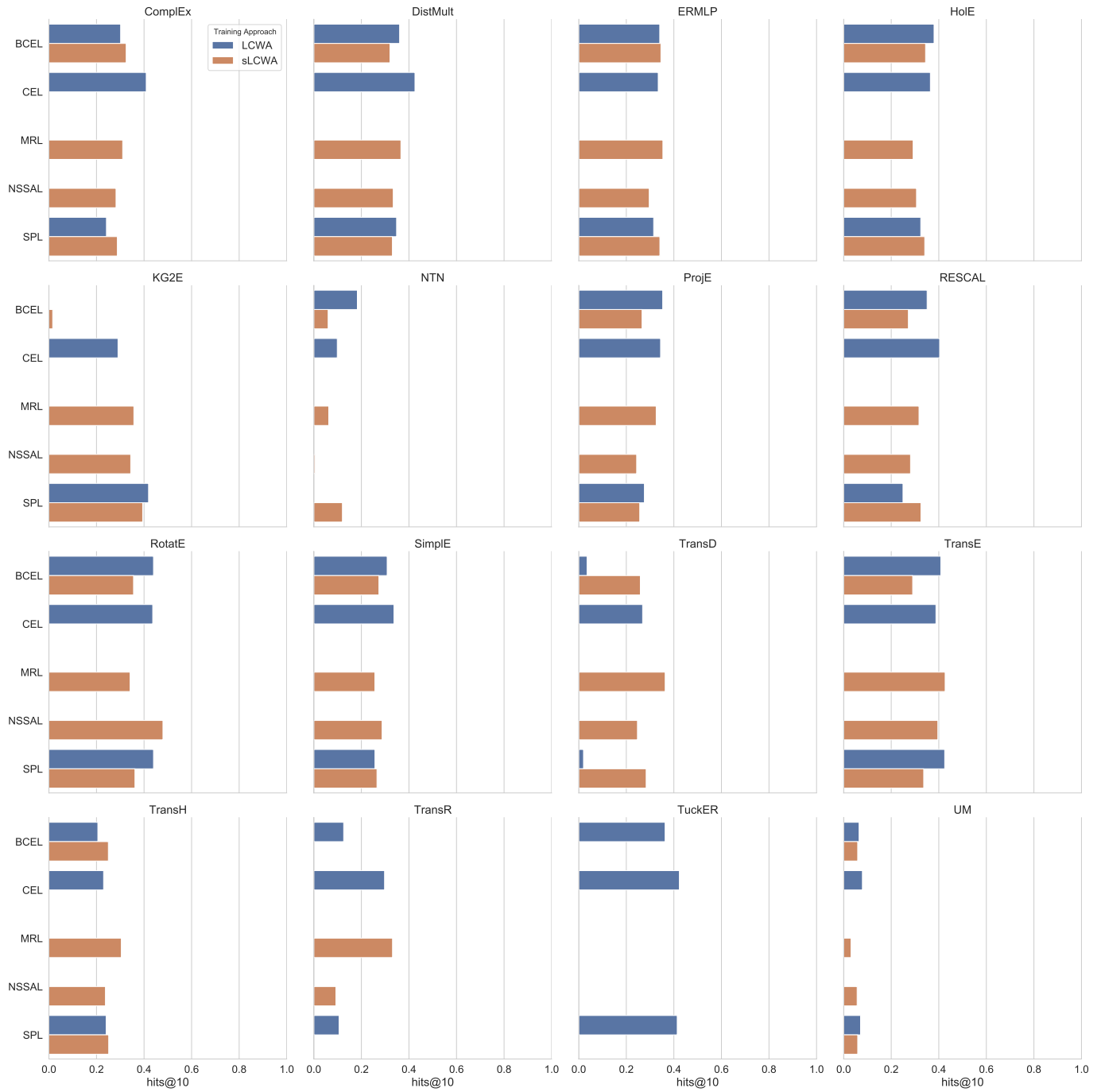


Fig. 34. Impact of the training approach on the performance for a fixed interaction model and loss function for the FB15K-237 dataset (results are aggregated based on the medians). **BCEL** refers to the binary cross entropy loss, **CEL** to the cross entropy loss, **MRL** to the margin ranking loss, **NSSAL** refers to the negative sampling self-adversarial loss, **SPL** to the softplus loss, **LCWA** to the local closed world assumption training approach and **sLCWA** to the stochastic local closed world assumption training approach.